Deep-Sea Research Part I 131 (2018) 101–120

Contents lists available at ScienceDirect

Deep-Sea Research Part I

journal homepage: www.elsevier.com/locate/dsri

Food-web complexity across hydrothermal vents on the Azores triple junction

Marie Portail[a,*], Christophe Brandily[b], Cécile Cathalot[c], Ana Colaço[d], Yves Gélinas[a], Bérengère Husson[b], Pierre-Marie Sarradin[b], Jozée Sarrazin[b]

[a] GEOTOP and Chemistry and Biochemistry Department, Concordia University, Montréal, Canada
[b] IFREMER, Centre de Bretagne, REM/EEP, Laboratoire Environnement Profond, F-29280 Plouzané, France
[c] IFREMER, Centre de Bretagne, REM/GM, Laboratoire Cycles Géochimiques et Ressources, F-29280 Plouzané, France
[d] MARE, Marine and Environmental Sciences Centre, Universidade dos Açores, Departamento de Oceanografia e Pescas, Horta, Açores, Portugal

ARTICLE INFO

Keywords:
Mid-Atlantic Ridge
Hydrothermal vents
Food webs
Stable isotopes
Functional traits

ABSTRACT

The assessment and comparison of food webs across various hydrothermal vent sites can enhance our understanding of ecological processes involved in the structure and function of biodiversity. The Menez Gwen, Lucky Strike and Rainbow vent fields are located on the Azores triple junction of the Mid-Atlantic Ridge. These fields have distinct depths (from 850 to 2320 m) and geological contexts (basaltic and ultramafic), but share similar faunal assemblages defined by the presence of foundation species that include *Bathymodiolus azoricus,* alvinocarid shrimp and gastropods. We compared the food webs of 13 faunal assemblages at these three sites using carbon and nitrogen stable isotope analyses (SIA). Results showed that photosynthesis-derived organic matter is a negligible basal source for vent food webs, at all depths. The contribution of methanotrophy versus autotrophy based on Calvin-Benson-Bassham (CBB) or reductive tricarboxylic acid (rTCA) cycles varied between and within vent fields according to the concentrations of reduced compounds (e.g. CH_4, H_2S). Species that were common to vent fields showed high trophic flexibility, suggesting weak trophic links to the metabolism of chemosynthetic primary producers. At the community level, a comparison of SIA-derived metrics between mussel assemblages from two vent fields (Menez Gwen & Lucky Strike) showed that the functional structure of food webs was highly similar in terms of basal niche diversification, functional specialization and redundancy. Coupling SIA to functional trait approaches included more variability within the analyses, but the functional structures were still highly comparable. These results suggest that despite variable environmental conditions (physico-chemical factors and basal sources) and faunal community structure, functional complexity remained relatively constant among mussel assemblages. This functional similarity may be favoured by the propensity of species to adapt to fluid variations and practise trophic flexibility. Furthermore, the different pools of species at vent fields may play similar functions in the community such as the change in composition does not affect the overall functional structure. Finally, the absence of a relationship between the functional structure and taxonomic diversity as well as the high overlap between species' isotopic niches within communities indicates that co-occuring species may have redundant functions. Therefore, the addition of species within in a functional group does not necessarily lead to more complexity. Overall, this study highlights the complexity of food webs within chemosynthetic communities and emphasizes the need to better characterize species' ecological niches and biotic interactions.

1. Introduction

Food-web studies — still in their infancy at hydrothermal vents — assess energy transfers within and between ecosystems, species ecological niches, biotic interactions, as well as the relationships between community structure and ecosystem functioning (Govenar, 2012). Vent food webs can be complex. In addition to inputs from the ocean surface (photosynthesis-derived organic matter (OM)), local primary production involves various chemosynthetic pathways (Hügler and Sievert, 2011; Karl, 1995) among which thiotrophy and methanotrophy usually dominate (ex.: Conway, 1994; Levin and Michener, 2002a). Consumers include symbiotic species, detritivores, bacterivores, scavengers, parasites and predators as well as migrant species (Bergquist et al., 2007; Govenar, 2012; Tunnicliffe, 1991). Although some consumers are

---

[*] Correspondence to: L-SP 265-24, Richard J. Renaud Science Complex, 7141 Sherbrooke W., Montréal, Canada.
E-mail address: marie.anoa.portail@gmail.com (M. Portail).

https://doi.org/10.1016/j.dsr.2017.11.010
Received 11 April 2017; Received in revised form 2 October 2017; Accepted 24 November 2017

highly specialized (Govenar et al., 2015; Levin et al., 2016), the trophic flexibility of many heterotrophic species suggests a high degree of generalism (Bell et al., 2016; Levin et al., 2009; Portail et al., 2016). In deep-sea chemosynthetic ecosystems, predation pressure seems relatively low (Bergquist et al., 2007; Portail et al., 2016; Van Dover and Fry, 1994), and many studies have confirmed that habitat and/or trophic partitioning are important structuring processes at the community scale (Beinart et al., 2012; Cordes et al., 2010c; Govenar et al., 2015; Levesque et al., 2003; Levin et al., 2015, 2013; Portail et al., 2016). Therefore, species coexistence in vent communities is most likely driven by a species sorting model. Accordingly, metacommunity models predict that isolated ecosystems with low diversity and heterogeneous environmental conditions — such as hydrothermal vents — tend to follow niche models in contrast to continuous ecosystems with high diversity and homogeneous environmental conditions — such as deep-sea photosynthesis-based ecosystems — that tend to correspond to a neutral model (Gage, 2004; Gravel et al., 2006). In addition to interspecific competition, positive biotic interactions, such as facilitation and mutualism, are assumed to be well developed in vents, with evidence that foundation species play a major role in structuring communities.

The Azores triple junction (in the northern Mid-Atlantic Ridge (MAR)) hosts several hydrothermal vent fields that are characterized by different geological contexts. The Menez Gwen (MG) and Lucky Strike (LS) vent fields are controlled by magmatic processes and found in a basaltic substrata while Rainbow (RB) is under tectonic control in an ultramafic lithology (review by Fouquet et al., 2013). These geological contexts together with the distinct depths, ranging from 850 to 2320 m, lead to different fluid chemistries in the three fields (Charlou et al., 2002, 2000). Active areas of the vent fields are colonized by two or three types of faunal assemblages defined by the visual dominance of either *Bathymodiolus azoricus* mussels, alvinocarid shrimps or, more recently discovered, small gastropods (Desbruyères et al., 2000; Desbruyères et al., 2001; Sarrazin et al., in preparation). These faunal assemblages are distributed according to their exposure to fluid flow and site morphology. At LS and MG, swarms of shrimp assemblages surrounding the hot fluids occur in close vicinity to emission sites (~ 0–1 m), mussels are found at greater distances from the emissions sites (~ 25 cm to 3 m) on rock surfaces (Cuvelier et al., 2009; Marcon et al., 2013) and gastropods in intermediate habitats on friable substratum (Sarrazin et al., in preparation). Variation in faunal community structure across vent fields can be related to a series of factors including the physical mechanisms that connect or isolate them, local physico-chemical conditions, biological processes as well as habitat instability (see review in Baker et al., 2010). Many of the potential influencing factors are interconnected, making it difficult to discriminate their respective contributions. Environmental factors can be classified as exogenous (e.g. biogeographical barriers, depth, distance) or endogenous (e.g. fluid physico-chemistry, substratum nature) to vents, thus providing a simplified context. Comparisons of similar faunal assemblages across vent fields can be used to discount, at least partially, factors related to the engineering role of foundation species and to their positions along the fluid-flux gradient. By doing so, the focus hones in on the role of endogenous factors related to the geological settings of vent fields against all exogenous factors. A recent study, based on this approach, supports the predominant role of exogenous factors in structuring the diversity and species composition of the macrofaunal community associated with *B. azoricus* (Sarrazin et al., in preparation). Among these factors, depth explains more variance than the geographical distance between vent fields, as previously suggested for other sites of the MAR (Rybakova and Galkin, 2015). To date, trophic studies in northern MAR vents have concentrated mainly on the foundation species, *B. azoricus* (Colaco et al., 2009; Detree et al., 2016; Martins et al., 2008; Ponnudurai et al., 2016; Riou et al., 2010a, 2010b, 2008) and *Rimicaris exoculata* shrimp (Allen et al., 2001; Pond et al., 1997; Ponsard et al., 2013; Rieley et al., 1999; Zbinden et al., 2004) whereas studies at the community level are scarce and relatively descriptive (Colaço et al., 2002a, 2007; De Busserolles et al., 2009). Methods that are now available to assess food-web complexity at the community level have never been applied to MAR vents.

Food webs were studied using stable isotope analyses (SIA, e.g. δ^{13}C and δ^{15}N signatures) that are highly valuable to define the “realized” ecological niche of species taking both trophic and habitat variables in consideration (Bearhop et al., 2004; Dubois and Colombo, 2014; Newsome et al., 2007). At the community level, functional metrics extracted from the overall δ^{13}C-δ^{15}N isotopic space are used to address food-web complexity and to estimate niche diversification at the base of the food web, the number of trophic levels, as well as functional diversity, specialization and redundancy (Cucherousset and Villéger, 2015; Jackson et al., 2011; Layman et al., 2007; Rigolet et al., 2015). In addition, to improve our understanding of the functional structure of communities, coupling SIA to functional trait analyses provides access to additional species functions. At the community level, metrics extracted from the multidimensional space of species functional traits can

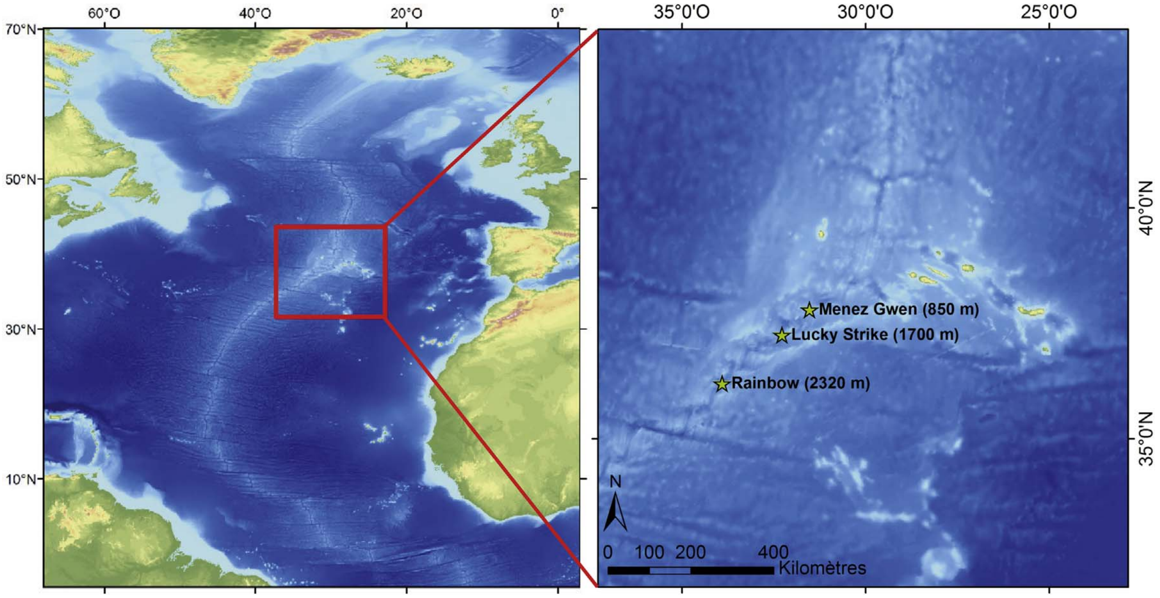

Fig. 1. Location of the study sites on the Azores triple junction.

Table 1
Abbreviations and locations of the studied assemblages.

Vent field	Edifice/site	Depth	Assemblage	Latitude	Longitude	Sample name	Sampled surface
Menez Gwen	MG3	850 m	Mussels (MG_M)	37°50.678' N	31°31.145' W	MG_{M1}	288 ± 17 cm^2
						MG_{M2}	431 ± 16 cm^2
						MG_{M3}	390 ± 11 cm^2
			Gastropods (MG_G)	37°50.679'N	31°31.138' W	MG_{G1}	230 ± 48 cm^2
						MG_{G2}	146 ± 18 cm^2
Lucky Strike	Eiffel Tower	1700 m	Mussels (LS_M)	37°17.347' N	32°16.526' W	LS_{M1}	442 ± 103 cm^2
						LS_{M2}	333 ± 90 cm^2
						LS_{M3}	308 ± 13 cm^2
Rainbow	France 5	2320 m	Mussels (RB_M)	36°13.766' N	33°54.118' W	RB_{M1}	–
	Flores			36°13.769' N	33°54.167' W	RB_{M2}	–
	Termitiere			36°13.773' N	33°54.174' W	RB_{M3}	–
	France 5	2320 m	Shrimps (RB_S)	36°13.767' N	33°54.117' W	RB_{S1}	–
	Termitiere			36°13.773' N	33°54.173' W	RB_{S2}	–

Table 2
Variability of environmental conditions across studied habitats from Menez Gwen (mussels: MG_M and gastropods: MG_G), Lucky Strike (mussels: LS_M) and Rainbow (mussels: RB_M and shrimps: RB_S).

	Mussel assemblage inter-field	Intra-field MG	Intra-field RB
Fluid flux	$RB_M \approx MG_M \approx LS_M$	$MG_G > MG_M$	$RB_S > RB_M$
[CH_4]	$RB_M > > MG_M > LS_M$	$MG_G > MG_M$	$RB_M > RB_S$
Metal concentrations	$RB_M > > LS_M > MG_M$	$MG_G > MG_M$	$RB_S > RB_M$
Expected [H_2S] availability	$LS_M > MG_M > > RB_M$	–	$RB_S > RB_M$
[NO_3^-]max	$LS_M > RB_M > MG_M$	$MG_G > MG_M$	$RB_S > RB_M$
[NH_4^+]max	$MG_M > RB_M > LS_M$	$MG_M > MG_G$	$RB_M > RB_S$

be used to estimate functional richness, evenness and divergence (Villéger et al., 2008). Functional traits can reflect the adaptation of species to their environment as well as their ecological functions that influence *in fine* ecosystem functions and services (Bremner, 2008; de Bello et al., 2010). This approach is relatively new to marine ecology in general, extremely scarce in the deep sea and almost absent from chemosynthetic ecosystems with, to date, only one study at methane seeps (Levin et al., 2016).

This study aims to assess and compare the functional structure of faunal communities of the northern MAR through an integrated approach based on SIA and functional trait analyses in relation to community structure and environmental condition patterns. The following questions are specifically addressed: (1) what are the basal sources on which species rely in the different faunal assemblages?; (2) what are the species trophic guilds and which inter-specific relationships can be highlighted? and (3) how does functional complexity, based on SIA and functional traits, vary between assemblages?

2. Materials and methods

2.1. Study design

2.1.1. Sampling sites

The BIOBAZ cruise was held in August 2013 on board the oceanographic research vessel *Pourquoi pas?* equipped with the *Victor6000* submersible. Three hydrothermal-vent fields located on the Azores triple junction on the Mid-Atlantic Ridge (MAR) were studied (Fig. 1): Menez Gwen (MG, 37°50.5′N, 31°31.5′W, 850 m), Lucky Strike (LS, 37°17.5′N, 32°16′W, 1700 m) and Rainbow (RB, 36° 13.8' N, 33°54.2' W, 2320 m).

Faunal sampling and environmental design followed the strategy described in Sarrazin et al. (2015). Assemblage locations, abbreviations and sampled surfaces are listed in Table 1. Three mussel assemblages characterized by the visual dominance of *Bathymodiolus azoricus* were studied within each vent field, MG (MG_{M1}, MG_{M2}, MG_{M3}), LS (LS_{M1}, LS_{M2}, LS_{M3}) and RB (RB_{M1}, RB_{M2}, RB_{M3}). The three assemblages were sampled at the same location within MG and LS but were sampled on different edifices within RB due to the sparse distribution of mussels at this vent field. Two gastropod assemblages defined by the visual dominance of *Lepetodrilus atlanticus* and *Protolira valvatoides* were studied at MG (MG_{G1} and MG_{G2}, as replicates) and two shrimp swarms defined by the dominance of *Rimicaris exoculata* were studied at RB (RB_{S1} and RB_{S2}, two distinct edifices). Samples taken at MG and LS can be considered quantitative because the surfaces sampled can be estimated accurately using imagery (see protocol in Sarrazin et al., 1997), but those from RB were sampled on vertical edifice walls thus preventing precise surface estimation.

On board, faunal samples were sorted over 20 µm, 250 µm and 1 mm sieves. Five individuals of each macrofaunal taxon and pools of 10–20 individuals of the dominant meiofaunal taxa were pre-sorted and frozen (−80 °C) for SIA. The remaining faunal samples were preserved in 96% ethanol and individuals identified back in the laboratory. The distinction between macrofauna and meiofauna was made according to taxonomic groups, not size. Macrofaunal identification generally reached the species level, but meiofaunal identification was often limited to the genus level.

2.1.2. Assemblage description

Environmental conditions and community structure of assemblages, that will be further detailed in Sarrazin et al., (in preparation), are summarized below.

2.1.2.1. Environmental conditions. Environmental variability across assemblages are presented in Table S1 and summarized in Table 2.

2.1.2.1.1. Inter-field variability. Mussel habitats were located in areas of low diffuse flow characterized by relatively low temperature (ΔT = 0–2 °C) and pH (ΔpH = 0–1 pH unit) anomalies. The chemical composition strongly discriminated MG_M and LS_M from RB_M, in accordance with their geological contexts (MG, LS: basaltic, RB: ultramafic) (Charlou et al., 2002). The first two sites were characterized by low concentrations of methane and metals (Mn, Fe) compared with RB_M. Although hydrogen sulphide concentrations were not been successfully acquired, trends can be inferred through iron concentrations because iron is known to precipitate hydrogen sulphide into sulphur iron minerals (Charlou et al., 2002; Le Bris and Duperron, 2010; Luther et al., 2001). Therefore, lower hydrogen sulphide availability was expected at RB_M compared with MG_M and LS_M. This hypothesis was further supported by the observation of a dense cover of orange ferrous deposits at RB_M (pers. obs.) and corroborates previous comparative studies of these vent fields (review by Le Bris and Duperron, 2010). Although MG_M and LS_M have more similar chemical environments, variations between the two were observed, in accordance with those found in the literature (maximal $[CH_4]$ at MG_M and maximal concentrations of metals at LS_M) (Charlou et al., 2002).

2.1.2.1.2. Intra-field variability. Within MG, the closer proximity of MG_G to fluid emissions compared with MG_M was reflected in higher temperatures, $[CH_4]$ and $[Mn_d]$ and lower pH values. Within RB, the higher influence of fluid emissions at RB_S than at RB_M was reflected in higher temperatures, $[Mn_d]$ and $[Fe_d]$ and lower pH whereas $[CH_4]$ was lower at RB_S. Higher fluid intensity at RBs suggests that H_2S availability was higher. Regarding nitrogen sources, intra-habitat variability was high and patterns of maximal concentrations differed (Table 2).

2.1.2.2. Community structure. The macrofaunal composition and diversity in the epifaunal assemblages (mussels & gastropods) showed a clear distinction of MG relative to LS and RB. Alpha diversity was higher at LS_M and RB_M compared with MG_M, and MG_G diversity was reduced compared to MG_M (Fig. S1A). Faunal assemblage composition mainly discriminated LS_M and RB_M from MG_M and MG_G (Fig. S1B); MG assemblages were characterized by a dominance of *P. valvatoides* and *L. atlanticus* gastropods, RB_M had higher dominance of *Amathys lutzi*, spionid polychaetes and *Mirocaris fortunata* shrimps and LS_M had higher dominance of *Branchipolynoe seepensis*, the commensal polynoid of *B. azoricus*, dorvilleids, and nemerteans. Dissimilarities of mussel assemblages across vents were mainly related to species turnover whereas those between mussel and gastropod assemblages of MG were related to nestedness. The dominant meiofaunal groups varied, with co-dominance of nematodes and copepods at LS_M, dominance of copepods at MG_M and MG_G and dominance of nematodes at RB_M.

2.1.3. Stable isotope analyses

2.1.3.1. Faunal samples. In the laboratory, frozen-preserved individuals were first rinsed in distilled Milli-Q water. For large specimens, muscle tissue and symbiotic organ, if present, were selected. For intermediate-size specimens, gut content was removed and for small specimens, the whole body was used for analysis. For meiofaunal taxa, several specimens were pooled to reach the minimum required weight (0.1 mg). Sub-samples were freeze-dried and ground into a homogeneous powder using a ball mill. Samples were weighed precisely (0.4 ± 0.1 mg) in tin capsules for carbon and nitrogen isotope analyses. For samples containing carbonates (e.g. copepods, echinoderms, gastropods and malacostracans), a subset was acidified to remove inorganic carbon. Acidification was carried out by the addition of 0.1 M HCl, drop by drop, until effervescence ceased. The sample was then dried at 60 °C under a fume extractor to evaporate the acid. To prevent the loss of dissolved organic matter, acidified samples were not rinsed (Jaschinski et al., 2008). Faunal samples were analysed on a Flash EA 1112 elemental analyser coupled to a Thermo Scientific Delta V Advantage stable isotope ratio mass spectrometer (EA-IRMS). Analytical precision based on the standard deviation of replicates of internal standards was ≤ 0.1‰ for both $\delta^{13}C$ and $\delta^{15}N$.

2.1.3.2. Water samples. $\delta^{13}C$ analyses of methane and carbon dioxide were carried out on a SSIM-CRDS isotopic analyser (PicarroG2201i) from the head-space phase of the water collected by the PEPITO water sampler a few cm above the faunal assemblages. All values are expressed in δ (‰) notation with respect to VPDB ($\delta^{13}C$) and air ($\delta^{15}N$): $\delta X\ (‰) = [(R_{sample}/R_{standard}) - 1] \times 10^3$, where X is either ^{13}C or ^{15}N, R_{sample} is the $^{13}C/^{12}C$ or $^{15}N/^{14}N$ isotope ratio of the sample and $R_{standard}$ is the $^{13}C/^{12}C$ or $^{15}N/^{14}N$ isotope ratio of the VPDB standard ($\delta^{13}C$) or air ($\delta^{15}N$).

2.2. Basal source context for stable isotope analyses

2.2.1. $\delta^{13}C$

Potential dominant basal sources in the three vent fields are related to four different $\delta^{13}C$ signals (Table 3) corresponding to photosynthesis-derived OM and local primary producers: autotrophs using the Calvin-Benson-Bassham (CBB) cycle or the reductive tricarboxylic acid (rTCA) cycle as well as methanotrophs. The $\delta^{13}C$ signatures of local primary producers depend on the isotopic values of their carbon sources and their isotopic fractionation during carbon fixation. Carbon dioxide in the studied assemblages had $\delta^{13}C$ values that were comparable between vent fields and closely related to values expected for ambient seawater (ΣCO_2 in the ocean: −2 to 2‰) (Zeebe and Wolf-Gladrow, 2001). Therefore, $\delta^{13}C$ ranges for CBB- and rTCA-autotrophs from the literature can be used. Autotrophs using the CBB cycle (e.g. *Gammaproteobacteria*, *Alphaproteobacteria* and *Zetaproteobacteria*) are associated with depleted $\delta^{13}C$ (−36 to −30‰) and those using the rTCA cycle (e.g. *Epsilonproteobacteria* and *Deltaproteobacteria*) with enriched $\delta^{13}C$ (−15 to 10‰) (Emerson et al., 2007; Hügler and Sievert, 2011; Kato et al., 2009). While thiotrophy is usually considered as the main metabolism of CBB and rTCA autotrophs, they may utilize other less well-known metabolisms such as hydrogen, ammonium and Fe^{2+} oxidation (Hügler and Sievert, 2011). Some bacteria are also able to use different energy sources, such as the thiotrophic endosymbionts of *B. azoricus* (Gammaproteobacteria) that can use both sulphur (sulphide and thiosulphate) and hydrogen (H_2) (Petersen et al., 2011; Ponnudurai et al., 2016). Methane $\delta^{13}C$ in the studied assemblages varied with higher methane $\delta^{13}C$ values at LS compared with MG and RB. Methanotrophic producers usually assimilate methane with little or no carbon-isotope fractionation and are thus defined by the methane $\delta^{13}C$ value (Alperin et al., 1988; Brooks et al., 1987; Feng et al., 2015; Fisher, 1990; Kennicutt et al., 1992b; Martens et al., 1999).

Table 3
$\delta^{13}C$ ratios of the potentially dominant basal sources in the studied vent fields. * no site differences.

Basal source	$\delta^{13}C$	References
Photosynthesis-derived organic matter	−24 to −22‰	(Gebruk et al., 2000; Khripounoff et al., 2001)
$\delta^{13}C$ (CO_2)	−4.4 to 2.5‰*, n = 25	Our study
Autotrophs/thiotrophs using the CBB cycle	−36 to −30‰	(Cavanaugh et al., 1992; Conway et al., 1994; Hügler and Sievert, 2011; Sievert et al., 2008; Trask and Van Dover, 1999)
Autotrophs/thiotrophs using the rTCA cycle	−15 to −10‰	(Hügler and Sievert, 2011; Sievert et al., 2008)
Methanotrophs (methane $\delta^{13}C$)	LS: −12.9 ± 3.4‰, n = 10 MG: −19.4 ± 1.8‰, n = 11 RB: −19.2 ± 3.5‰, n = 4	Our study in accordance with (Charlou et al., 2002)

Table 4
δ^{15}N ratios of the potentially dominant basal sources in the studied vent fields (* indicate significant variation among samples of an assemblage). Assemblages from Menez Gwen (mussels: MG_M and gastropods: MG_G), Lucky Strike (mussels: LS_M) and Rainbow (mussels: RB_M and shrimps: RB_S).

Basal source	δ^{15}N	References
Photosynthetic-derived organic matter	4–6‰	(Gebruk et al., 2000; Khripounoff et al., 2001)
Endosymbionts (*B. azoricus* gills)	LS_M: −11.1 ± 1.8‰, n:13* MG_M: −10.1 ± 1.3‰, n:15 RB_M: −4.5 ± 1.9‰, n:15 MG_G: −2.3 ± 1.6‰, n:3 RB_S: −2.9 ± 0.2‰, n:3	Our study
Ectosymbionts (*R. exoculata* cephalothorax)	RB_S: 5.2 ± 0.6‰, n:8*	Our study
Filamentous bacteria (*Beggiatoa* spp.)	LS_M: −2.5 ± 0.1‰, n:2	Our study

2.2.2. $\delta^{15}N$

δ^{15}N ratios are not expected to vary among basal sources, but in chemosynthetic ecosystems and in MAR vent fields they do (Table 4). First, the δ^{15}N signature of photosynthesis-derived OM is enriched compared with local producers due to its degradation in the water column. However, the δ^{15}N of local producers can also vary in particular according to biogeochemical gradients and especially the abundance of nitrogen sources along sediment profiles in vent and seep sedimentary assemblages (Bourbonnais et al., 2012; Portail et al., 2016; Southward et al., 2001). Endosymbiont compartments are represented in *B. azoricus*, which rely on two types of *Gammaproteobacteria* endosymbionts hosted in the bacteriocytes of their gills: thiotrophs using the CBB cycle to fix CO_2 and methanotrophs type I using methane as energy and carbon sources (Duperron et al., 2006; Fiala-Medioni et al., 2002; Robinson et al., 1998; Spiridonova et al., 2006; Won et al., 2003). Ectosymbionts are represented in the *R. exoculata* cephalothorax, forming filamentous mats that are dominated by rTCA-thiotrophic *Epsilonproteobacteria* (Hügler et al., 2011). Finally, free-living microbes are found as filamentous microbial mats dominated by thiotrophic *Beggiatoa* spp., *Gammaproteobacteria* that can develop on *B. azoricus* shells (Crepeau et al., 2011) and on any available surface. The endosymbiotic species *B. azoricus* showed the most depleted δ^{15}N values of all assemblages and variation across assemblages was high (from ~ −11 to −2‰). Filamentous microbial mats in LS_M had δ^{13}C signatures consistent with thiotrophs using the CBB cycle but were significantly enriched in ^{15}N compared with *B. azoricus*, with a shift of 8.5‰. Similarly, ectosymbionts of *R. exoculata* had δ^{13}C signatures corresponding to rTCA-autotrophy but had enriched δ^{15}N compared with *B. azoricus* in RB_{S2}, with a shift of 8.6‰. These results suggest that the free-living microbial pool and ectosymbionts may be characterized by distinct δ^{15}N signatures relative to those of *B. azoricus* endosymbiont compartments.

2.3. Data analyses

2.3.1. Baseline

Due to the δ^{15}N spatial variability of primary producers, faunal δ^{15}N isotope data must be corrected for baseline variations to allow comparisons across assemblages (Post, 2002). While free-living microbes are likely the main basal sources for heterotrophic fauna, they remain difficult to sample. Because *B. azoricus* was present in all assemblages, it can be used as a δ^{15}N baseline correction when comparing isotopic taxa across assemblages. Despite the presence of multiple baselines, previously introduced (Section 2.2.2), the consistent shift of ~8.5‰ between microbial mats and *B. azoricus* endosymbionts seem to indicate that these baselines are similarly affected across assemblages. To assess whether *B. azoricus* represents a good correction factor, correlations between δ^{15}N of *B. azoricus* and associated heterotrophic fauna were tested. In addition, δ^{15}N relationships between *B. azoricus* gill and muscle were explored. Differences between endosymbiotic (gill) and aposymbiotic (muscle) tissues may highlight variable fractionation factors of consumers toward sources depending on environmental conditions.

2.3.2. Mixing models

Although stable isotope mixing models are increasingly used to quantify consumer diets, their use was not possible in our study owing to the presence of a large number of potential sources (three main sources associated with four δ^{13}C signals and multiple δ^{15}N baselines). Therefore, only trends of the predominant basal sources within assemblages will be discussed. The only exception was *Bathymodiolus azoricus* for which a SIAR mixing model (Parnell et al., 2008) was used to estimate the relative contribution of thiotrophy and methanotrophy. Although experimental studies have demonstrated that *B. azoricus* can feed on particulate organic matter (POM) and that mussels and their symbionts may rely on dissolved organic matter (DOM) (Riou et al., 2010b, 2010c), these strategies are assumed to be secondary (De Busserolles et al., 2009). POM and DOM are composed of a mixture of photosynthesis-derived and chemosynthesis-derived OM and studies agree on the negligible role of photosynthesis-derived OM to the *B. azoricus* diet (De Busserolles et al., 2009; Riou et al., 2010b; Salerno et al., 2005).

2.3.3. Faunal trophic guilds

Trophic guilds were classified into symbiont hosts, bacterivores, detritivores/scavengers, commensals and predators, with the bacterivorous trophic guild referring to deposit feeders specialized in the consumption of microbes (Bergquist et al., 2007, Table S2). Trophic guild assignments were based on data from the literature when available. For the other species or families with unknown trophic guilds or multiple guild assignments according to where they have been studied, trophic guild was assigned by comparing stable isotope ratios between species and between species and basal sources. Consumers were identified based on an enrichment (from consumer to source) of 3.4‰ for δ^{15}N and 1‰ for δ^{13}C (Conway et al., 1994), taking into account the intraspecific isotope variability. Discrimination of predators from detritivores/scavengers based on δ^{15}N signatures is not always efficient (Jumars et al., 2015). Species that belong to families with known predator species were classified as predators only when potential prey could be identified.

2.3.4. Food-web metrics

The structure of food-webs at the community level was first described using Layman's community-wide metrics (Layman et al., 2007). A Bayesian approach allowed for the propagation of sampling error

Table 5
Resume of Layman's Bayesian food-web metrics with their acronyms and interpretation.

Acronym	Metric	Interpretation
SEAs	Small sample-size-corrected standard ellipse areas (SEAc) + Bayesian standard ellipse area (SEAb).	Overall extent of food web
CR	Carbon range ($\Delta\delta^{13}$C)	Basal niche diversification
NR	Nitrogen range ($\Delta\delta^{15}$N)	Trophic length
CD	Mean distance to the centroid (average Euclidian distance of each species component to the centroid)	Average trophic specialization
CVNND	Coefficient of variation of the nearest neighbour distance (ratio of the standard deviation to the mean of nearest neighbour distance)	Trophic redundancy

Table 6
Resume of functional metrics with their acronyms and interpretation.

Acronym	Metric	Interpretation	Calculation
IRic	Isotopic richness	Global functional richness	Convex hull area without taking into account species biomass
IDiv	Isotopic divergence	Degree of trophic specialization	Degree to which the distribution of species in an isotopic space maximizes the divergence
IDis	Isotopic dispersion	Average of trophic specialization (CD)	Estimate of the weighted deviation of the mean position of the points relative to the maximum distance from the centre
IEve	Isotopic evenness	Trophic redundancy	Regularity in distribution of species and their weight along the shortest tree that connects the dots
IUni	Isotopic uniqueness	Trophic redundancy	Inverse of the average isotopic redundancy where isotopic redundancy reflects the average approximation of species in the isotopic space.

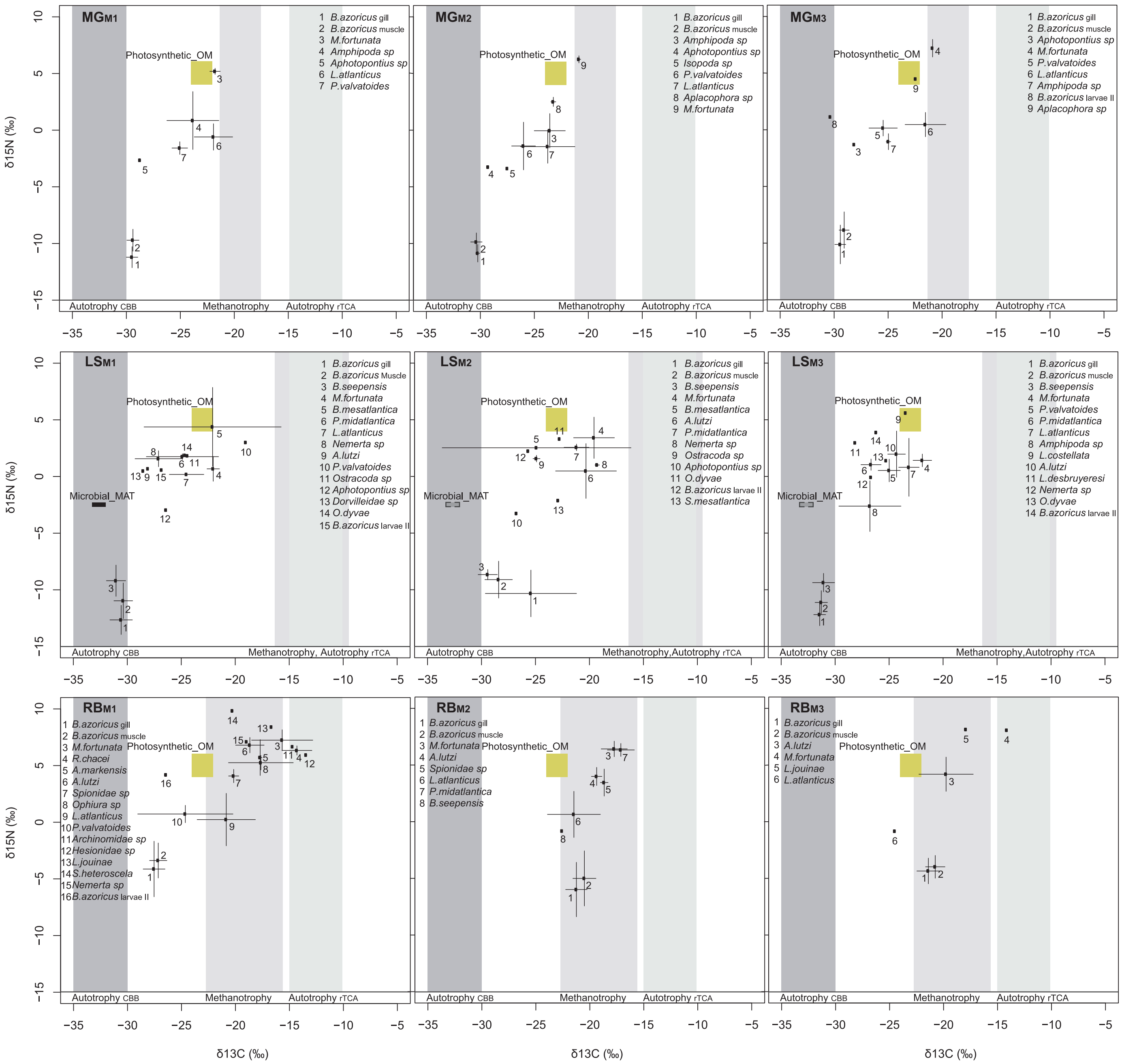

Fig. 2. Biplots of carbon ($\delta^{13}C$) and nitrogen ($\delta^{15}N$) signatures (mean ± SD) of consumers and food resources in mussel assemblages from Menez Gwen (MG_{M1}, MG_{M2}, MG_{M3}), Lucky Strike (LS_{M1}, LS_{M2}, LS_{M3}) and Rainbow (RB_{M1}, RB_{M2}, RB_{M3}) vent fields. Isotopic signatures of photosynthesis-derived organic matter (photosynthetic_OM) are shown in green. Local producers $\delta^{13}C$ ranges are shown in the three shaded areas; their $\delta^{15}N$ signatures are unknown. (For interpretation of the references to color in this figure legend, the reader is referred to the web version of this article).

related to the estimations of mean stable isotope ratios for community components (Jackson et al., 2011). Carrying over this error provides a measurement of uncertainty and is less affected by variation in the number of community components. To compare metrics among assemblages, the δ^{13}C signature ranges of possible basal sources must be similar (Layman et al., 2007), which is a valid hypothesis here with autotrophs using the CBB or rTCA cycles that characterize the δ^{13}C ranges of basal sources within all assemblages. Layman's Bayesian metrics are defined in Table 5 with trophic redundancy metrics updated by Brind'Amour and Dubois (2013). Metrics were calculated and compared using the siber.hull.metrics function from the Stable Isotope Analysis in the R package (SIAR; Parnell and Jackson, 2013; Parnell et al., 2010). Standard ellipse areas (SEAs) were calculated and compared using the SIAR and Stable Isotope Bayesian Ellipses packages (SIBER; Jackson et al., 2011).

The food-web structures were also described using functional metrics taking into account the relative biomass of species within communities (Cucherousset and Villéger, 2015; Rigolet et al., 2015). *B. azoricus* and its commensal polynoid dominate biomass in assemblages but have limited to no trophic links with the rest of the faunal community (De Busserolles et al., 2009). They were thus excluded from our analyses. For each assemblage, the roles of species were weighted by using their respective mean biomass (Table S3) multiplied by their density (Sarrazin et al., in preparation). Functional metrics are defined in Table 6. The confidence interval of each index was calculated using a bootstrap method (nrep = 1000).

2.3.5. *Functional structure*

While SIA are used to characterize species' "realized" trophic niches, ecological niches are also shaped by other biological traits that influence the functions of species and *in fine* ecosystem functioning and services (Bremner, 2008; Clark, 2016; de Bello et al., 2010; de Juan et al., 2015). A functional trait analysis was carried out using qualitative or quantitative variables available at the species level. These traits include carbon source (δ^{13}C as a proxy), trophic level (δ^{15}N), trophic diet (bacterivore, detritivore, carnivore), trophic strategy (suspensivore, deposivore, predator), size (megafauna, macrofauna, meiofauna) and mobility (tube-forming, crawler, swimmer). Building on the most recent analytical and statistical approaches, metrics extracted from the multidimensional space of functional traits at the community-scale were used to compare assemblage functioning (Mouchet et al., 2010). The confidence interval of each index was calculated by a bootstrap method performed on SIA measurements.

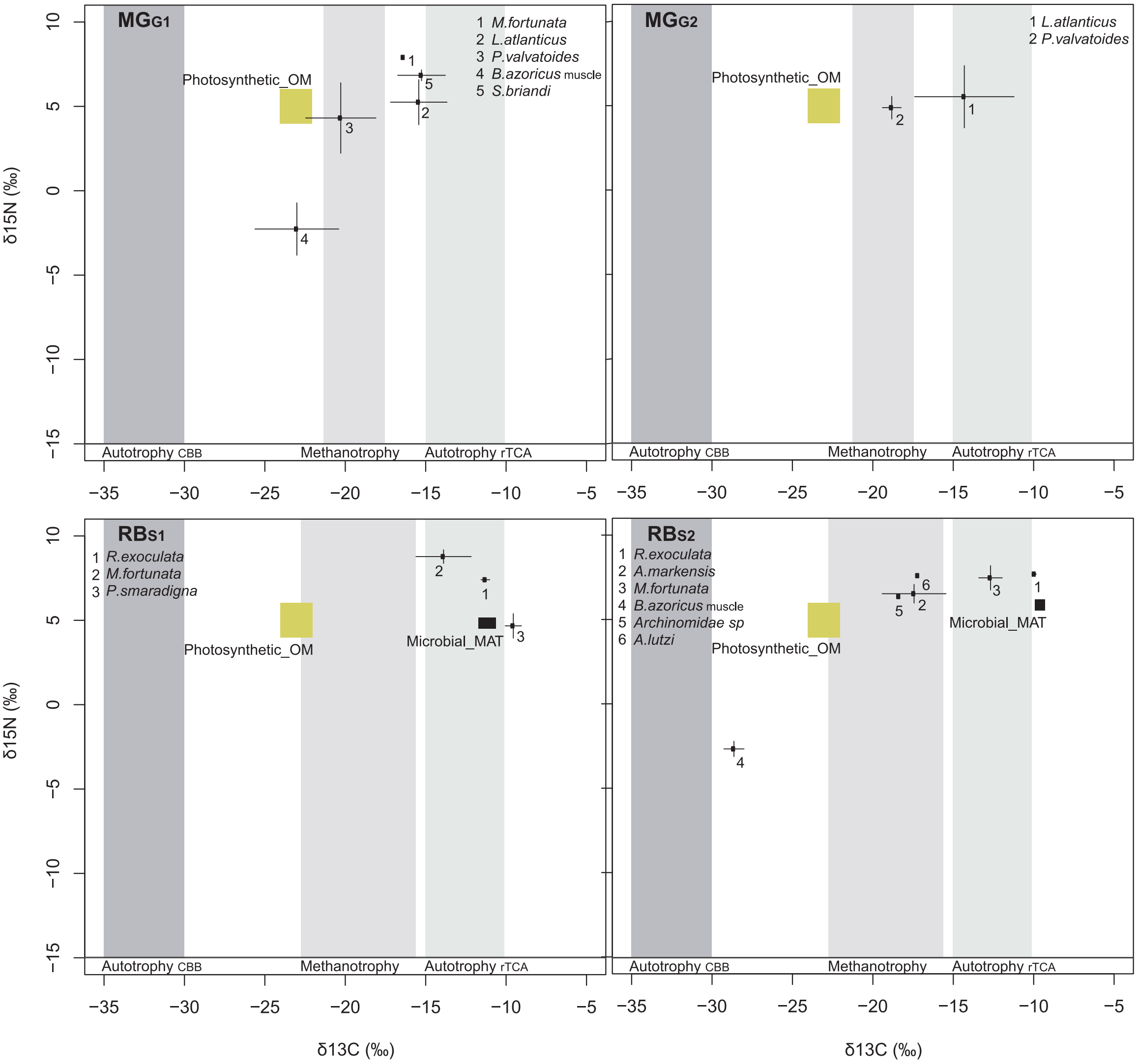

Fig. 3. Biplots of carbon (δ^{13}C) and nitrogen (δ^{15}N) signatures (mean ± SD) of consumers and food resources in gastropod assemblages from Menez Gwen (MG_{G1}, MG_{G2}) and shrimp assemblages from Rainbow (RB_{S1}, RB_{S2}) vent-fields. Isotopic signatures of photosynthesis-derived organic matter (photosynthetic_OM) are shown in green. Local producers δ^{13}C ranges are shown in the three shaded areas; their δ^{15}N signatures are unknown. (For interpretation of the references to color in this figure legend, the reader is referred to the web version of this article).

3. Results

$\delta^{13}C$ and $\delta^{15}N$ ratios of sources and consumers are shown in Fig. 2 for mussel assemblages and in Fig. 3 for the other assemblages (gastropods and shrimp). Within epifaunal assemblages (mussel and gastropods), isotopic data were available for most of the macrofaunal community (from 91% to 100% of the total density) and on dominant meiofaunal taxa: *Aphotopontius* sp. copepods at LS and MG, *Oncholaimus dyvae* nematodes (description in progress, Zeppilli unpublished data.) and ostracods at LS. Species' trophic guilds known from the literature and isotopic data are listed in Table S2.

3.1. Basal sources

3.1.1. Community-wide description

3.1.1.1. Photosynthetic versus chemosynthetic OM. In all assemblages, photosynthesis-derived organic matter (photosynthetic-OM) was not identified as a dominant source because most taxa had $\delta^{15}N$ lower than this basal source (Figs. 2 and 3). For the few taxa that showed ^{15}N enrichment compared to photosynthetic-OM (i.e. RB_M, RB_S, MG_G), their $\delta^{13}C$ signatures were strongly enriched compared with this source, suggesting a diet based on local chemosynthetic production.

3.1.1.2. Faunal $\delta^{13}C$. Mean faunal $\delta^{13}C$ values were comparable between samples within an assemblage ($MG_{M1} = MG_{M2} = MG_{M3}$, $LS_{M1} = LS_{M2} = LS_{M3}$, $RB_{M1} = RB_{M2} = RB_{M3}$, $MG_{G1} = MG_{G2}$, $RB_{S1} = RB_{S2}$, Table S2) but were significantly different between assemblages (RB_S, MG_G, RB_M, LS_M, MG_M, $p < 0.001$). Faunal $\delta^{13}C$ were significantly enriched at RB_S (−15.4 ± 5.9‰), MG_G (−17.6 ± 3.2‰) and RB_M (−19.4 ± 3.6‰) compared with LS_M (−25.2 ± 3.2‰) and MG_M (−25.4 ± 3.2‰) ($p < 0.05$). Contributions of enriched $\delta^{13}C$ sources (methanotrophy and rTCA-autotrophy), compared with the more $\delta^{13}C$ depleted sources (CBB-autotrophy), appeared to be higher in the former group (RB_S, MG_G, RB_M) than in the latter (LS_M, MG_M). Although contributions of methanotrophy and rTCA-autotrophy cannot be easily distinguished, environmental data (Section 2.2) suggested that enriched faunal $\delta^{13}C$ in RB_M are linked to methanotrophy and enriched faunal $\delta^{13}C$ in RB_S to rTCA-autotrophy and likely thiotrophy. Among mussel assemblages, higher methane concentrations were observed in RB_M than in MG_M and LS_M and hydrogen sulphide supposedly followed the opposite pattern. Within the RB vent field, $[CH_4]$ at RB_S was more reduced than at RB_M, making it comparable to MG_M and LS_M, but hydrogen sulphide availability was theoretically higher than that at RB_M. In the MG vent field, MG_G reached relatively high methane concentrations compared with RB_M, suggesting that methanotrophy may be involved in the enrichment of faunal $\delta^{13}C$.

3.1.1.3. Faunal $\delta^{15}N$. Mean faunal $\delta^{15}N$ signatures were not significantly different between samples within an assemblage but the inter-assemblage variability was significant ($p < 0.001$). The patterns were similar to those of $\delta^{13}C$ with mean faunal $\delta^{15}N$ significantly enriched at RB_S (6.0 ± 3.4‰), MG_G (4.6 ± 3.3‰) and RB_M (3.9 ± 4.1‰) relative to LS_M (−0.5 ± 4.6‰) and MG_M (−0.9 ± 4.8‰) ($p < 0.05$). These results may represent inter-assemblage baseline variation (availability and isotopic variability of inorganic nitrogen sources used by primary producers), variable contributions of photosynthetic and chemosynthetic OM between assemblages as well as variable dominance of species trophic levels and specialization on chemoautotroph microbes for detritivores. No relationships between faunal $\delta^{15}N$ and nitrate or ammonium concentrations were observed.

3.1.2. $\delta^{15}N$ baseline variations

3.1.2.1. Bathymodiolus azoricus. Within the RB vent field, there were no significant differences in $\delta^{15}N$ of *B. azoricus* according to tissues or samples ($p > 0.05$). Within the MG and LS vent fields, $\delta^{15}N$ of *B. azoricus* differed between tissues ($\delta^{15}N_{gill} < \delta^{15}N_{muscle}$) and samples (p: 0.007; $MG_{M1} = MG_{M2} = MG_{M3} < MG_{G1}$, p: 0.03; $LS_{M1} = LS_{M3} < LS_{M2}$) with no significant interaction of the two factors (unbalanced two-way ANOVA). Despite these variations, mean $\delta^{15}N$ of *B. azoricus* differed significantly between assemblages ($p < 0.001$). *B. azoricus* showed a $\delta^{15}N$ enrichment at MG_G (−2.3 ± 1.6‰), RB_S (−2.9 ± 0.2‰) and RB_M (−4.5 ± 1.9‰) compared with MG_M (−10.1 ± 1.3‰) and LS_M (−11.1 ± 1.8‰) assemblages ($p < 0.05$). Such $\delta^{15}N$ variation across samples and assemblages for an endosymbiotic species may reflect the variability of primary producer $\delta^{15}N$, thus reflecting baseline variation.

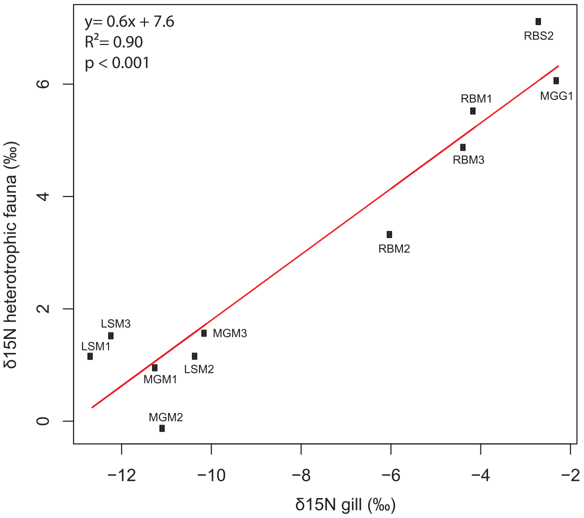

Fig. 4. Correlation between the $\delta^{15}N$ signature of *Bathymodiolus azoricus* gills and the mean faunal $\delta^{15}N$ signature of the rest of the community for all each assemblage studied (mussel assemblages from Menez Gwen (MG_{M1}, MG_{M2}, MG_{M3}), Lucky Strike (LS_{M1}, LS_{M2}, LS_{M3}) and Rainbow (RB_{M1}, RB_{M2}, RB_{M3}) as well as one gastropod assemblage (MG_{G1}) from Menez Gwen and one shrimp assemblage (RB_{S2}) from Rainbow).

3.1.2.2. Baseline. The use of the $\delta^{15}N$ values of *B. azoricus* as a correction factor for other taxa was tested. The correlation between the mean $\delta^{15}N$ signatures of *B. azoricus* gills and that of associated fauna per assemblage was significant ($R^2 = 0.90$, $p < 0.001$, Fig. 4). These results suggest that $\delta^{15}N$ variation in heterotrophic fauna is directly or indirectly related to the local baseline rather than to the relative abundance of photosynthetic-OM, which varies with depth.

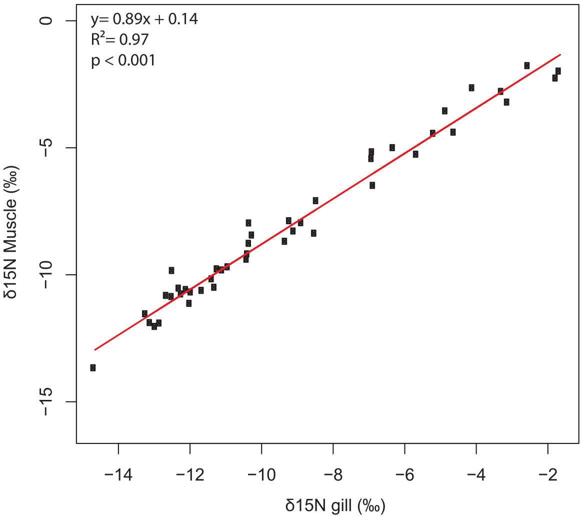

Fig. 5. Correlation between muscle and gill $\delta^{15}N$ signatures from *Bathymodiolus azoricus* sampled at the three vent fields.

Heterotrophs mainly rely on free-living basal sources, suggesting that $\delta^{15}N$ variation between local baselines of assemblages (chemoautotroph microbial mats and *B. azoricus* endosymbionts) may be relatively similar among assemblages. These results are in accordance with the consistent $\delta^{15}N$ shift observed between *B. azoricus* and microbial mats in LS and RB, estimated at 8.5‰ (Section 2.4.1). In addition, a correlation between *B. azoricus* $\delta^{15}N_{gill}$ and $\delta^{15}N_{muscle}$, based on all *B. azoricus* individuals for which isotopic data were available on both tissues simultaneously (44 individuals, from the three vent fields), showed a highly significant relationship ($R^2 = 0.97$, $p < 0.001$, Fig. 5). The relatively low $\delta^{15}N$ differences between gills and muscles were consistent across assemblages of the three vent fields, suggesting that *B. azoricus* isotopic fractionation with respect to endosymbiotic bacteria was similar despite environmental variation. These two correlations found for $\delta^{15}N$ values thus show that *B. azoricus* can be used to correct for faunal $\delta^{15}N$ baseline variations. To compare $\delta^{15}N$ of taxa between assemblages, the following correction was used: $|\delta^{15}N_{consumer} - \delta^{15}N_{B.\ azoricus}|$.

3.1.2.3. *Corrected $\delta^{15}N$*.

At the assemblage scale, mean faunal $\delta^{15}N$ values after baseline corrections ($\delta^{15}N_c$) were still not significantly different between samples within an assemblage but were significantly different between assemblages ($p = 0.001$). Mean faunal $\delta^{15}N_c$ values were significantly higher at LS_M (11.4 ± 4.6‰) than at RB_S (8.2 ± 4.0‰), MG_G (6.7 ± 4.0‰) and RB_M (8.6 ± 3.9‰, $p < 0.05$), MG_M was intermediate between these two groups (9.9 ± 4.5‰). Lower $\delta^{15}N_c$ indicate that taxa in communities had lower trophic levels and/or greater specialization on chemoautotrophic microbes for detritivores.

3.1.3. *Trophic flexibility of shared species*

3.1.3.1. *Endosymbiotic mussel $\delta^{13}C$*.

Within each vent field, the $\delta^{13}C$ of *B. azoricus* did not vary by tissue type (gill vs. muscle) but by sample ($p < 0.001$; $MG_{M2} < MG_{M1} = MG_{M3} < MG_{G1}$, $p < 0.001$; $LS_{M3} < LS_{M1} < LS_{M2}$, $p < 0.001$; $RB_{S2} < RB_{M1} < RB_{M2} = RB_{M3}$), with no significant interaction of the two factors (unbalanced two-way ANOVA). Differences in *B. azoricus* $\delta^{13}C$ between assemblages were significant ($p < 0.001$): *B. azoricus* from RB_M (−23.1 ± 3.2‰) and MG_G (−23.0 ± 2.6‰) had enriched $\delta^{13}C$ compared with MG_M (−29.7 ± 0.7‰), LS_M (−29.6 ± 2.6‰) and RB_S (−28.7 ± 0.8‰) ($p < 0.05$).

3.1.3.2. *Mixing model SIAR*.

Estimations of basal source contributions to the *B. azoricus* diet within MG_M and LS_M led to comparable results, with higher contributions of CBB-thiotrophy (80–90%) than methanotrophy (10–20%) (Fig. 6A). Within RB_M, the *B. azoricus* diet was more balanced, with methanotrophy being slightly dominant (60%) over CBB-thiotrophy (40%). Within MG_G and RB_S, the few *B. azoricus* found had diets different to those found in the mussel-dominant assemblages of their respective vent fields (Fig. 6A, B). *B. azoricus* from MG_G appeared to benefit from methanotrophy and CBB-thiotrophy in equivalent proportions whereas *B. azoricus* from the RB_S showed a higher contribution of CBB-thiotrophy (80%) than methanotrophy (20%).

3.1.3.3. *Relationship with environmental conditions*.

A correlation between methane concentrations and the calculated contribution of methanotrophy to the diet of *B. azoricus* was significant ($p < 0.01$, R^2: 0.88 for n:5), confirming the flexibility of the *B. azoricus* trophic diet according to concentrations of chemical compounds. This result also supports the previous assumptions made at the community level, with enriched mean $\delta^{13}C$ in MG_G being related to higher contributions from methanotrophs than from rTCA thiotrophs, similar to RB_M (Section 3.1.1).

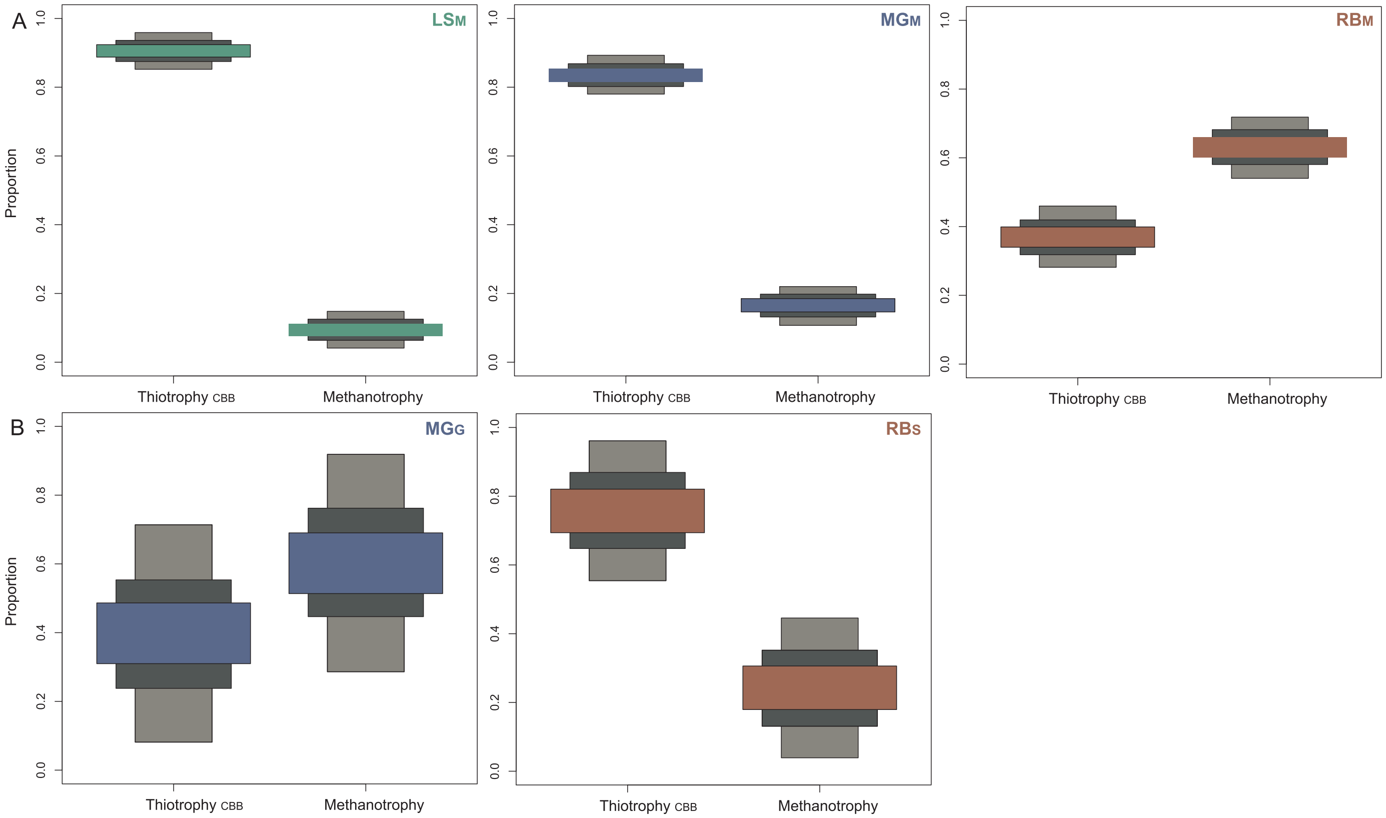

Fig. 6. Relative contributions of methanotrophy and thiotrophy using the CBB cycle to the *Bathymodiolus azoricus* diet within (A) mussel assemblages from Lucky Strike (LS_M), Menez Gwen (MG_M) and Rainbow (RB_M) and (B) gastropod assemblages from Menez Gwen (MG_G) and shrimp assemblages from Rainbow (RB_S). The mixing model considered a $\delta^{13}C$ fractionation of 1 ± 0.4‰ from consumer toward sources.

Table 7

Intra- and inter-field variability of $\delta^{13}C$ and $\delta^{15}N_c$ signatures for species common to all assemblages. Assemblages from Menez Gwen (mussels: MG_{M1}, MG_{M2}, MG_{M3} and gastropods: MG_{G1} and MG_{G2}), Lucky Strike (mussels: LS_{M1}, LS_{M2}, LS_{M3}) and Rainbow (mussels: RB_{M1}, RB_{M2}, RB_{M3} and shrimps: RB_{S1} and RB_{S2}).

		$\delta^{13}C$ differences	Shift	p_val	$\delta^{15}N_c$ differences	Shift	p_val
Intra-fields							
MG	*Lepetodrilus atlanticus*	$MG_{M1}, MG_{M2}, MG_{M3} < MG_{G1}, MG_{G2}$	~ 7‰	< 0.001	$MG_{G1}, (MG_{M2}) < MG_{M1}, MG_{M3}, (MG_{M2})$	~ 2‰	0.008
	Protolira. valvatoides	$MG_{M1}, MG_{M2}, MG_{M3} < MG_{G1}, MG_{G2}$	~ 6‰	< 0.001	$MG_{G1} < MG_{M1}, MG_{M2}, MG_{M3}$	~ 3‰	0.005
	Amphipoda sp.	$MG_{M1} = MG_{M2} = MG_{M3}$	–	ns	$MG_{M3} < MG_{M1}, MG_{M2}$	2 to 3‰	0.05
LS	*Branchipolynoe seepensis*	$LS_{M1}, LS_{M3} < LS_{M2}$	~ 1‰	0.04	$LS_{M2}, (LS_{M3}) < LS_{M1}, (LS_{M3})$	~ 1‰	0.03
	Mirocaris fortunata	$LS_{M1}, LS_{M3} < LS_{M2}$	~ 2‰	0.05	$LS_{M1} = LS_{M3} = LS_{M2}$	–	ns
	Amathys lutzi	$LS_{M3} < LS_{M2}$	~ 4‰	0.02	$LS_{M2} < LS_{M3}$	~.3‰	0.05
	Pseudorimula midatlantica	$LS_{M1}, LS_{M3} < LS_{M2}$	4 to 6‰	0.02	$LS_{M2}, LS_{M3} < LS_{M1}$	~ 1‰	0.02
RB	*Amathys lutzi*	$RB_{M1} = RB_{M2} = RB_{M3}$	–	ns	$RB_{M3}, (RB_{M2}) < RB_{M1}, (RB_{M2})$	~ 2‰	0.05
	Spionidae sp.	$RB_{M1} < RB_{M2}$	~ 1‰	0.01	$RB_{M2} = RB_{M1}$	–	ns
	Lepetodrilus atlanticus	$RB_{M2} = RB_{M1}$	–	ns	$RB_{M2} = RB_{M1}$	–	ns
	Mirocaris fortunata	$RB_{M2},(RB_{M1}) < RB_{S1}, RB_{S2}, (RB_{M1})$	4 to 5‰	0.02	$RB_{S2} < RB_{M1} < RB_{M2}$	1 to 2‰	0.01
	Rimicaris exoculata	$RB_{S1} < RB_{S2}$	~ 1‰	< 0.001	no baseline correction at RB_{S1}		
Inter-fields							
Lepetodrilus atlanticus		$RB_M, MG_M, LS_M < MG_G$	~ 8‰	0.002	$RB_M, MG_G < MG_M < LS_M$	3 to 8‰	< 0.001
Protolira. valvatoides		$MG_M, (LS_M, RB_M) < (LS_M, RB_M), MG_G$	~ 6‰	0.004	$RB_M, MG_G < MG_M < LS_M$	6 to 8‰	< 0.001
Mirocaris fortunata		$MG_M, LS_M < RB_M < RB_S$	3 to 8‰	< 0.001	$RB_S < RB_M < LS_M < MG_M$	2 to 7‰	< 0.001
Pseudorimula midatlantica		$LS_M < RB_M$	~ 7‰	0.008	$RB_M < LS_M$	~ 1‰	0.04
Amathys lutzi		$LS_M < RB_M$	~ 4‰	0.02	$RB_M < LS_M$	~ 3‰	0.005
Amphipoda sp.		$MG_M = RB_M$.	–	ns	$MG_M = RB_M$.	–	ns

3.1.3.4. Heterotrophic species. Only a subset of species common to all assemblages was analysed with enough replicates to apply a mean comparison test of their isotopic ratios. Despite some variation between samples at LS_M, RB_M and RB_S, $\delta^{13}C$ differences between assemblages were significant for all but one species (Table 7). Enriched $\delta^{13}C$ signatures were generally associated with MG_G and RB_S, followed by RB_M and then MG_M and LS_M. This variability was similar to the pattern observed at the community level (Section 3.1.1) and suggested that shared fauna have trophic flexibility according to variation in basal sources. Despite significant differences in species' $\delta^{15}N_c$ signatures between samples (for 6 out of 11 species), most species still showed significant $\delta^{15}N_c$ differences between assemblages (5 out of 6 species, Table 7). This pattern suggests that species-specific $\delta^{15}N_c$ signatures discriminate RB_S with lower $\delta^{15}N_c$, from MG_G and RB_M and finally MG_M and LS_M assemblages. This variability is consistent with the observed community-level pattern (Section 3.1.2) and suggests that fauna common to all assemblages have variable degrees of trophic specialization on chemoautotrophic microorganisms.

3.2. Functional complexity

3.2.1. Trophic guilds

Species' trophic guilds included endosymbiotic species as well as potential bacterivorous specialists, detritivores/scavengers and predators (Table S2). In the literature, many species and families have been related to distinct trophic guilds according to the study site. Taking into account the potential issues related to SIA that will be discussed below (Section 4.2), potential trophic guilds were assigned to species within assemblages (Fig. 8).

3.2.1.1. Symbiotrophic assignment. Although *B. azoricus* derives its diet from its chemoautotrophic bacterial endosymbionts, the shrimp *Rimicaris exoculata* may not solely feed on its chemoautotrophic bacterial ectosymbionts and have been classified as facultative detritivores/scavengers. In our study, *R. exoculata* sampled in RB_S had similar $\delta^{13}C$ and slightly enriched $\delta^{15}N$ (2.6‰) compared with the ectosymbionts in their cephalothorax cavity, suggesting their predominant role in the shrimp diet. Interestingly, *Peltospira smaragdina* gastropods from RB_S had even more negative $\delta^{15}N$ than *R. exoculata*, highlighting a putative endosymbiotic relationship that has already been demonstrated for other species of the same genus (Table S2).

3.2.1.2. Commensal/parasite assignment. *Branchipolynoe seepensis* polynoids living inside *B. azoricus* mussels had $\delta^{13}C$ signatures comparable to their host and enriched in ^{15}N by 1–4‰ compared with *B. azoricus* muscle. A close relationship between *B. seepensis* and *B. azoricus* was thus apparent and both direct and indirect contributions of local POM (mixture of photosynthetic-POM, pseudofaeces, autotrophic and heterotrophic free-living microbes), which have enriched $\delta^{15}N$ and different $\delta^{13}C$ values, can be excluded. Nevertheless, the nature of the interaction between *B. seepensis* and *B. azoricus* remains uncertain. *B. seepensis* has long been considered commensal, but recent studies suggest that *B. azoricus* gills that host *B. seepensis* are damaged suggesting a potential semi-parasitic relationship (Table S2). The diet of *B. seepensis* may consist of predation on *B. azoricus* tissue or feeding on *B. azoricus* dead tissue or mucus.

3.2.1.3. Bacterivores versus higher consumers. Variations in *B. azoricus* $\delta^{15}N$ was assumed to reflect those of free-living microbial mats because the heterotrophic faunal community showed similar $\delta^{15}N$ variation as observed in *B. azoricus* (Section 3.1.3). The shift of +8.5‰ observed for chemoautotrophic microbial mats compared to *B. azoricus* muscle (LS_{M1}, RB_{S2}) was used to approximate the $\delta^{15}N$ signature of microbial mats in all assemblages. $\delta^{15}N$ enrichment of up to 3.4‰ is generally used to identify a consumer compared with its food source and was thus used here to distinguish bacterivores from higher consumer taxa. Numerous species appeared as highly specialized bacterivores, but the degree of specialization varied among them and between assemblages for species they had in common. Some species were even related to distinct trophic guilds according to the assemblage (*P. valvatoides*, *P. midatlantica*, *A. lutzi*, *M. fortunata*). Therefore, bacterivory did not appear as a strict trophic strategy but rather as a trophic preference.

3.2.1.4. Predators versus detritivores/scavengers. Predators were identified based on prey identification and behavioural observations. Based on SIA and the identification of potential prey, only a few species appeared to be predators (Fig. 7, Table 8). Among predators, except for *B. azoricus* larvae PII and *Segonzacia mesatlantica*, multiple potential prey were identified, that may reflect a generalist rather than a specialist feeding strategy.

Overall, the analysis of trophic guilds showed that detritivores including non-selective feeding strategies and bacterivorous specialists dominated all assemblages whereas a relatively low number of predators were identified (~ 5 taxa). Inter-assemblage variability of

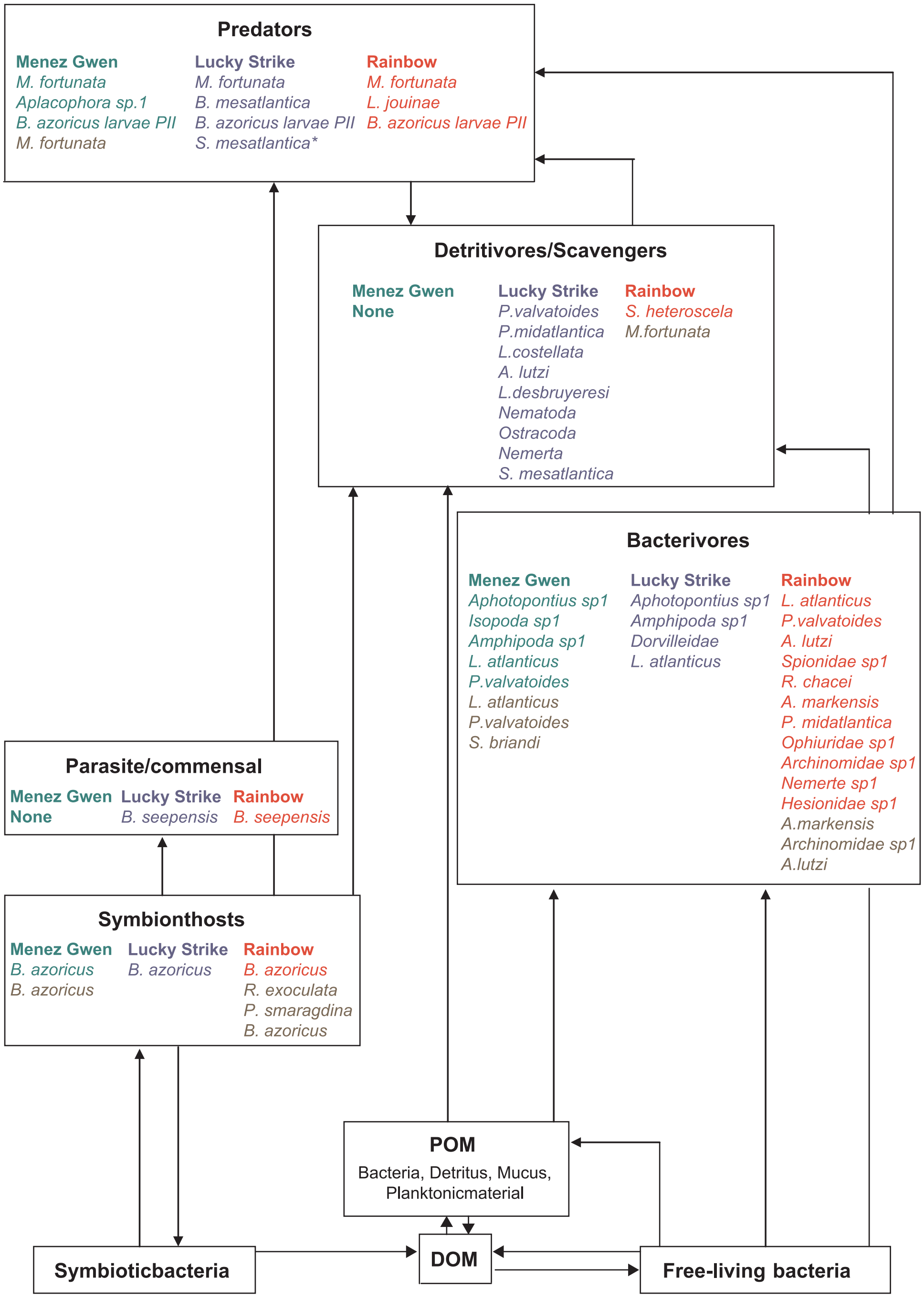

Fig. 7. Trophic guild assignments based on SIA, literature and behavioural analyses. * indicate that *Segonzacia mesatlantica* was identified as a mixotroph (detritivore and predator). Taxa from mussel assemblages in Menez Gwen are shown in green, Lucky Strike in purple and Rainbow in red. Taxa from high fluid-flux assemblages, gastropods from Menez Gwen and shrimps from Rainbow are shown in brown. (For interpretation of the references to color in this figure legend, the reader is referred to the web version of this article).

trophic guild dominance within macrofaunal communities revealed higher dominance of detritivores and “commensal/parasites” in LS_M, higher dominance of predators in RB_M and MG_M with MG_G being almost exclusively represented by bacterivores (Fig. 8).

3.2.2. *Food-web metrics*

Assemblages that benefited from quantitative sampling and for which sampled surfaces were comparable were used to compare the structure of food webs (LS_{M1}, LS_{M2}, LS_{M3}, MG_{M1}, MG_{M2}, MG_{M3}, sampled surface from 300 to 400 cm^2). Taxa included in these analyses correspond from 93% to 100% of the macrofaunal community, together with the dominant meiofaunal groups (copepods, nematodes and ostracods at LS and copepods at MG).

3.2.2.1. Layman's Bayesian metrics. Layman's Bayesian metrics within the samples of LS_M and MG_M are shown in Fig. 9 (see Table 5 for metric details). The small sample-size-corrected standard ellipse areas and the Bayesian standard ellipse area (SEAb) were comparable among LS_M and MG_M samples as well as between assemblages. Similarly, none the other metrics (carbon range (CR), nitrogen range (NR), mean distance to the centroid (CD) and coefficient of variation of the nearest neighbour distance (CVNND)) discriminated samples or assemblages. All together, these results suggest that the food web structure is similar between MG_M and LS_M.

3.2.2.2. Functional metrics, biomass dependant. Illustrations of functional metric calculations are shown in Fig. S2 and the results following bootstrap in Fig. 10 (see Table 6 for metric details). The isotopic richness (IRic) was comparable among samples in LS_M and MG_M assemblages and the inter-assemblage variability was not

Table 8
Predator/prey interactions identified at the different study sites. Assemblages from Menez Gwen (mussels: MG_M and gastropods: MG_G), Lucky Strike (mussels: LS_M) and Rainbow (mussels: RB_M and shrimps: RB_S).

Ass.	Predator	Potential prey
MG_M	*Mirocaris fortunata*	*Lepetodrilus atlanticus*, Amphipoda sp., Aplacophora sp.
	Aplacophora sp.	*Lepetodrilus atlanticus*, Amphipoda sp.
	Bathymodiolus azoricus larvae PII	*Aphotopontius* sp.
MG_G	*Mirocaris fortunata*	*Lepetodrilus atlanticus*
LS_M	*Mirocaris fortunata*	*Amathys lutzi*, Nemertean sp., *Lepetodrilus atlanticus*
	Branchinotogluma mesatlantica	Almost all fauna except *Bathymodiolus azoricus* and its commensal polychaete
	Bathymodiolus azoricus larvae PII	*Aphotopontius* sp.
	Segonzacia mesatlantica	*Bathymodiolus azoricus* + detritus including microbial mat (mixotrophy)
RB_M	*Mirocaris fortunata*	Spionidae sp., *Amathys lutzi*
	Lepidonotopodium jouinae	*Amathys lutzi, Alvinocaris markensis, Ophiura* sp.
	Bathymodiolus azoricus larvae PII	*Aphotopontius* sp.
RB_s	–	–

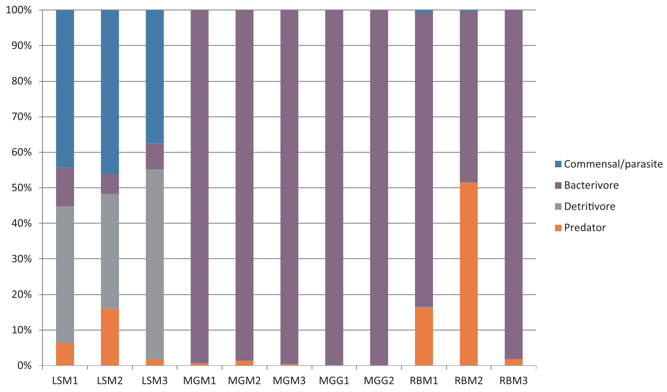

Fig. 8. Trophic guild dominance within macrofaunal communities of the studied assemblages. Mussel assemblages from Lucky Strike (LS_{M1}, LS_{M2}, LS_{M3}), Menez Gwen (MG_{M1}, MG_{M2}, MG_{M3}) and Rainbow (RB_{M1}, RB_{M2}, RB_{M3}) as well as gastropod assemblages from Menez Gwen (MG_{G1}, MG_{G2}).

significant. The isotopic divergence (IDiv) showed significant differences among LS_M and MG_M samples ($LS_{M1} < LS_{M2}$, LS_{M3} and $MG_{M2} < MG_{M1}$, $p < 0.05$), but the inter-assemblage variability was not significant. The isotopic dispersion (IDis) showed significant differences among LS_M samples ($LS_{M1} < LS_{M2}$, $p < 0.05$), but inter-assemblage variability was not significant. The isotopic evenness (IEve) showed significant differences among LS_M samples ($LS_{M2} < LS_{M3}$, $p < 0.05$), but the inter-assemblage variability was not significant. The isotopic uniqueness (IUni) showed significant differences among LS_M and MG_M samples ($LS_{M1} < LS_{M2}$, LS_{M3} and $MG_{M2} < MG_{M3}$), but the inter-assemblage variability was not significant. These results suggested some variance across assemblage samples but, similar to Layman's metrics, showed a similar food-web structures between MG_M and LS_M.

3.2.3. *Functional traits*

Metrics of the functional complexity are shown in Fig. 11. The overall functional richness (FRic) showed significant differences among LS_M and MG_M samples ($LS_{M1} > LS_{M3}$, $LS_{M3} > LS_{M2}$ and $MG_{M1} > MG_{M3}$, $p < 0.05$) and the difference between MG_M and LS_M assemblages was not significant. The functional dispersion (FDis) showed significant differences among LS_M and MG_M samples ($LS_{M3} > LS_{M1}$, LS_{M2} and $MG_{M2} > MG_{M1}$, MG_{M3}, $p < 0.05$) and the difference between assemblages was significant, with LS_M having higher functional dispersion than MG_M ($p < 0.05$). The functional evenness (FEve) showed significant differences among LS_M and MG_M samples (LS_{M1}, $LS_{M3} > LS_{M2}$ and $MG_{M2} > MG_{M3} > MG_{M1}$, $p < 0.05$), but the difference between MG_M and LS_M assemblages was not significant. Therefore, while some differences emerged among samples, no distinction at the assemblage-scale emerged with the exception of FDis.

4. Discussion

This food web study offers the opportunity to address the functioning of the northern MAR vent communities at the regional scale where both exogenous and endogenous factors can affect ecological processes and the structure of faunal communities.

4.1. *Basal sources*

The three vent fields studied here are located along a bathymetric gradient (850–2320 m depth) that drives many of the exogenous factors that may influence the functioning of these vent ecosystems, including trophic inputs from photosynthetic primary production. Nevertheless, and consistent with patterns observed in deep-sea chemosynthetic ecosystems (e.g. Carlier et al., 2010; Levin and Michener, 2002b; MacAvoy et al., 2008), photosynthesis-derived organic matter (photosynthetic-OM) proved to be a minor energy source in the food webs of active areas within the three vent fields. Similar conclusions were drawn from previous food-web studies on northern MAR vents (Colaço et al., 2002a, 2007; De Busserolles et al., 2009). In general, vent deep-sea fauna appear to be highly specialized on local chemosynthetic production, even in areas where photosynthetic inputs are exceptionally high such as the Guaymas Basin (Portail et al., 2016). Furthermore, photosynthetic-OM contributions at the MAR vents studied here did not vary with depth. Instead, variation in faunal $\delta^{13}C$ between vent fields was related to distinct contributions of local primary producers (methanotrophs, CBB- and rTCA-autotrophs). Accordingly, $\delta^{15}N$ values varied with the $\delta^{15}N$ of local primary producers. The $\delta^{15}N$ of heterotrophic fauna was significantly related to that of the endosymbiotic species *B. azoricus*, which represents the baseline in our study. We suggest that the lability of photosynthetic-OM in the deep sea needs to be assessed because this source has been shown to sustain vent endemic taxa in photic zones (Comeault et al., 2010; Stevens et al., 2015). For instance, photosynthetic-OM may rapidly become refractory during its descent in the water column. Therefore, photosynthetic-OM inputs, considered a potential exogenous factor, may not influence active vent communities through bottom-up control, in contrast to "regular" deep-sea habitats (Wei et al., 2010). Migrant predators may however depend on these inputs and endemic communities may thus still be indirectly affected through top-down control (Carney, 1994, 2005; Cordes et al., 2010b; Olu et al., 2010; Sahling et al., 2003).

Local chemosynthetic primary production is thus the predominant source of carbon fuelling our MAR vent assemblages. The dominant primary producers sustaining the food webs of the three vent fields were similar (methanotrophs and autotrophs using the CBB and rTCA cycles), but their contributions varied between assemblages among and between fields. Sources with enriched $\delta^{13}C$ (methanotrophs and autotrophs depending on the rTCA cycle) compared with the depleted signatures (autotrophs depending on the CBB cycle) had higher contributions in assemblages associated with higher fluid-flux (MG_G gastropods, RB_S shrimp and to a lesser extent RB_M mussels) than mussel assemblages from Menez Gwen (MG_M) and Lucky Strike (LS_M). The enrichment in $\delta^{13}C$ in the fauna located closer to fluid emissions is a recurrent observation (Colaço et al., 2002b; De Busserolles et al., 2009; Fisher et al., 1994; Govenar et al., 2015; Levesque et al., 2003; Levin et al., 2009; Limen and Juniper, 2006; O'Brien et al., 2015). According to environmental data and basal source contributions to *B. azoricus* diet (see below), rTCA-autotrophy and especially thiotrophy were identified as the source of enrichment in RB_S, whereas methanotrophy may

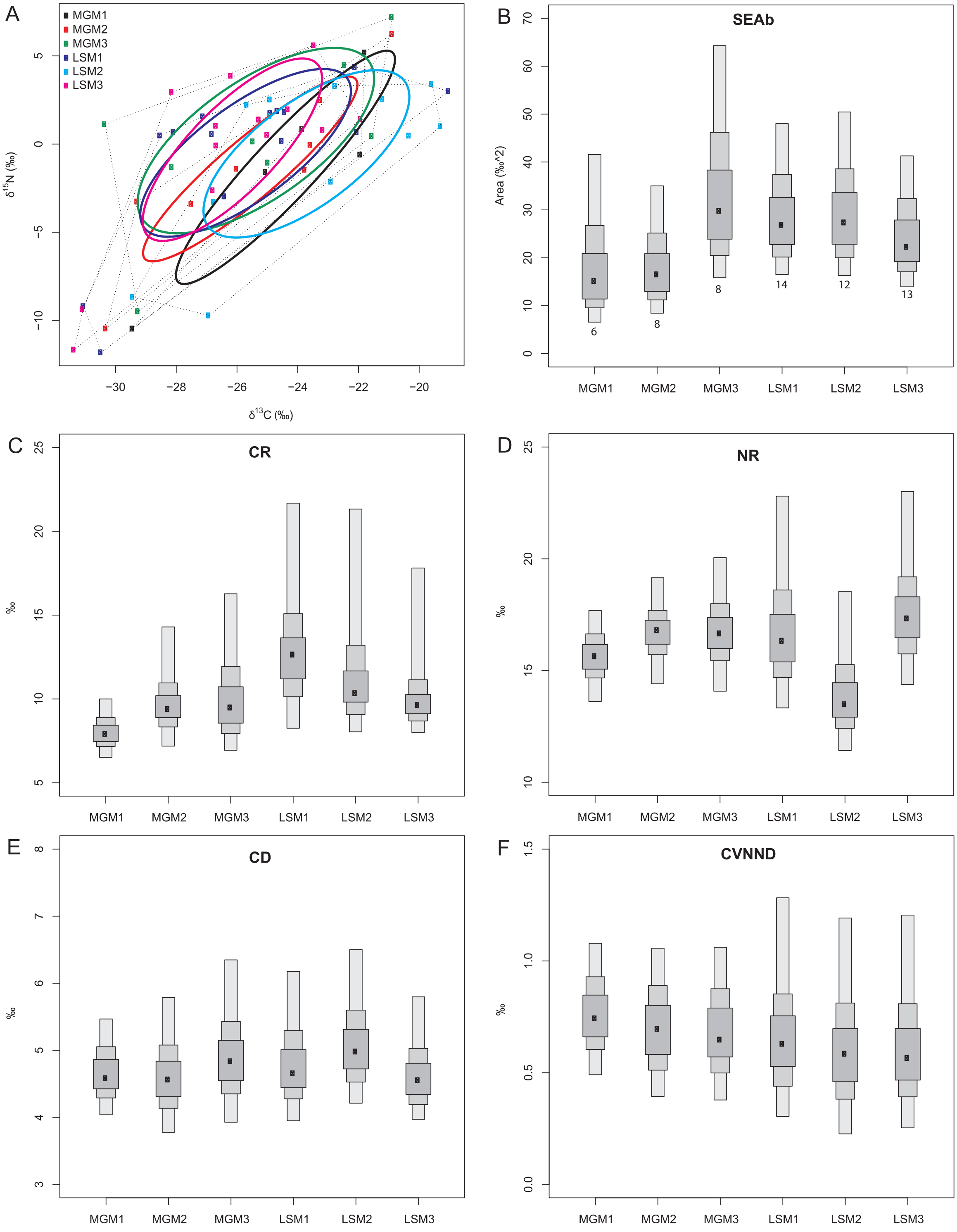

Fig. 9. Food web metrics of mussel assemblages from Menez Gwen and Lucky Strike vent fields. Standard ellipse areas: (A) Solid lines enclose the standard ellipse area (SEAc), containing ca. 40% of the data. (B) Density plots showing the credibility intervals of the Bayesian standard ellipse areas (SEAb). Numbers below boxes give the number of invertebrate species sampled. Bayesian results for the (C) δ^{13}C range, CR, (D) δ^{15}N range, NR (E) mean distance to centroid, CD, and (F) the coefficient of variation of the nearest neighbour distance, CVNND. Black dots are the modes and boxes indicate the 50%, 75% and 95% credibility intervals, from wide to narrow.

explain the enrichment in RB_M and MG_G. The rTCA cycle rather than CBB is known to be favoured under hypoxic conditions that are typical of RB_S habitats, which are located at the interface between cold oxygenated seawater and vent fluid emissions (Campbell et al., 2006; Hügler et al., 2005). Further evidence includes ectosymbiont communities of *Rimicaris exoculata* (dominant species of RB_S) that are dominated by thiotrophic *Epsilonproteobacteria* using the rTCA cycle (Hügler et al., 2011). Overall, our results underline the major role of environmental conditions (e.g. reduced compounds and oxygen) on the metabolism of microbial communities, leading to distinct dominant sources at the base of food webs. The contributions of these sources varied between vent fields according to their geological contexts and within vent fields according to fluid intensity. More studies and methods are needed to determine the food-web contributions of autotrophic

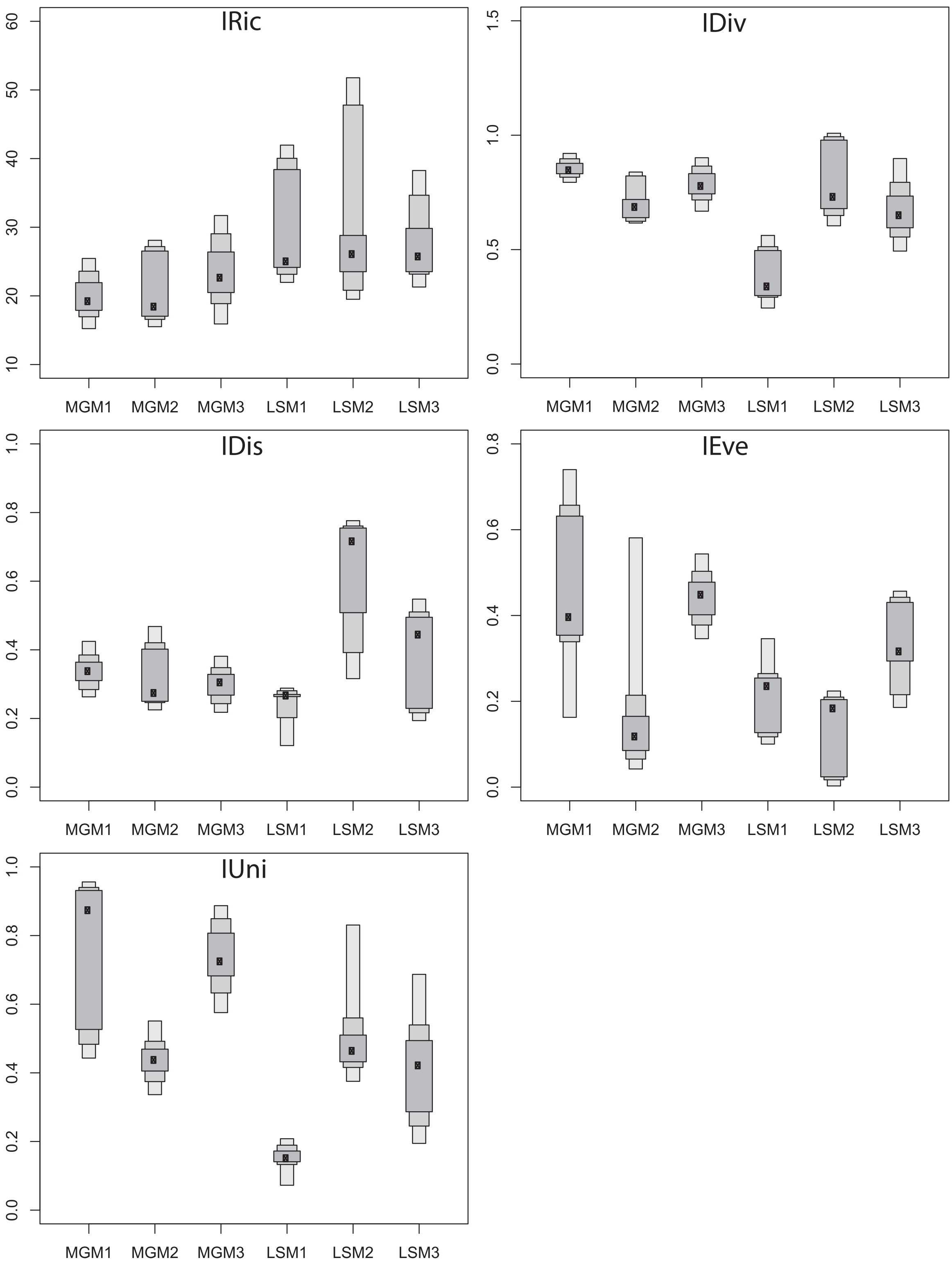

Fig. 10. Food-web metrics of mussel assemblages from Menez Gwen and Lucky Strike vent fields. Tested using the "bootstrap" method, black dots are the modes and boxes indicate the 50%, 75% and 95% credibility intervals, from wide to narrow.

metabolisms using the CBB and rTCA cycles, especially at RB where, in addition to hydrogen sulphide, the oxidation of iron, and potentially hydrogen may occur (Le Bris and Duperron, 2010; Schmidt et al., 2008).

Contributions of inorganic nitrogen sources to primary production within chemosynthetic food webs remain poorly defined (Portail et al., 2016; Van Dover, 2007). Raw faunal $\delta^{15}N$ reached depleted values as low as −10‰ that are assumed to be related to consumption of local inorganic nitrogen sources (Conway et al., 1994; Kennicutt et al., 1992a; Van Dover, 2007). Nitrates and especially ammonium resulting from OM decomposition are usually ^{15}N-depleted compared with oceanic nitrates (Hoch et al., 1992; Lee and Childress, 1996). In addition, inorganic nitrogen assimilation can lead to high isotopic fractionation in consumers with respect to sources (by up to ~30‰) especially

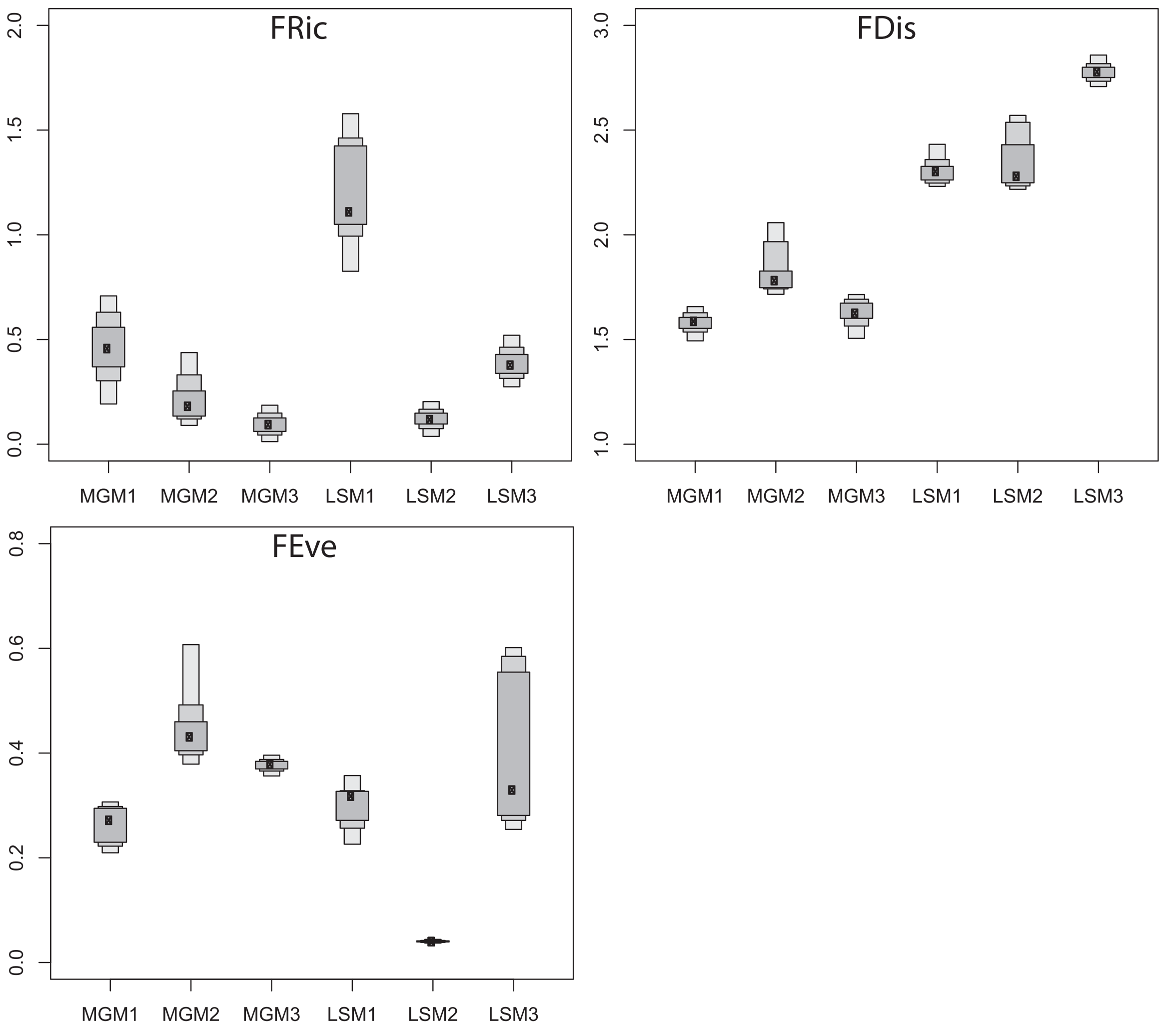

Fig. 11. Metrics of the functional complexity in mussel assemblages from Menez Gwen and Lucky Strike vent fields. Tested using the "bootstrap" method, black dots are the modes and boxes indicate the 50%, 75% and 95% credibility intervals, from wider to thinner.

when they display high concentrations (Hoch et al., 1992; Macko et al., 1987). *B. azoricus* $\delta^{15}N$ signatures were used as baseline values within assemblages and were shown to vary by up to 10‰ across assemblages. There was no relationship between *B. azoricus* $\delta^{15}N$ and bioavailable nitrogen source concentrations (i.e. NO_3^-, NH_4^+). However, dinitrogen (N_2) has not been measured. N_2 fixation is not assumed to be common in vent ecosystems because this strategy is usually initiated to overcome the limitation of bioavailable forms of nitrogen (Dixon and Kahn, 2004; Howarth et al., 1988). The identification of isotopic values of potential nitrogen sources would greatly benefit vent food web studies.

Heterotrophic fauna are suggested to mainly rely on free-living microbial sources whereas the contribution of endosymbiont pools may not be significant, because predation of endosymbiotic species is often considered to be negligible in vent assemblages (review by Govenar, 2012). Interestingly, chemoautotrophic microbial mat samples (*Beggiatoa* spp. or *R. exoculata* ectosymbionts) within this study, showed $\delta^{15}N$ enrichment of around 8.5‰ ($n = 3$) compared with *B. azoricus*. Such high differences between primary producers within assemblages may result from variable availability and isotopic signatures of nitrogen sources and/or distinct fractionation factors according to environmental conditions. For example, the endosymbionts found in *B. azoricus* gills are highly isolated from the ambient environment where microbial mats develop. Furthermore, endosymbionts may assimilate isotopically light nitrate or ammonium excreted by their hosts (Bode et al., 2014; Rodrigues et al., 2013) that also may reach relatively high concentrations in mussel beds. The consistent $\delta^{15}N$ shift between microbial mats and endosymbiotic bacteria as well as the significant relationship between $\delta^{15}N$ of *B. azoricus* and heterotrophic fauna across assemblages suggest that free-living microbes may experience baseline variation similar to that in *B. azoricus*. These multiple co-occuring baselines are assumed to reflect distinct microhabitats and smaller spatial variation may occur within the free-living compartments according to biogeochemical gradients. Overall, our results provide further support that, in chemosynthetic ecosystems, primary production is tightly linked to local nitrogen sources that are influenced by biogeochemical processes acting at small spatial scales (Bourbonnais et al., 2012; Conway, 1994; Portail et al., 2016).

The presence of species that are common across assemblages raises questions about their reliance on specific basal sources. The $\delta^{13}C$ and corrected $\delta^{15}N$ variability of common species were relatively comparable to patterns observed at the community level, suggesting that these species exhibit high trophic flexibility. Although the presence of a large number of potential sources limited the study to trends of predominant basal sources, stable isotope mixing models were used, knowing that the *B. azoricus* diet mainly depends on two types of endosymbionts hosted in their gills (thiotrophic *Gammaproteobacteria* using the CBB cycle and methanotrophic bacteria) (Duperron et al., 2006; Fiala-Medioni et al., 2002; Robinson et al., 1998; Spiridonova et al., 2006; Won et al., 2003). Our results showed a strong relationship between the concentrations of reduced compounds and the contribution of endosymbionts to the *B. azoricus* diet (i.e. methane concentrations and relative methanotrophic contributions). Previous studies have demonstrated high spatial variability of endosymbiont proportions in *B. azoricus* at multiple scales (inter-fields, intra-field, intra-edifice) (Colaço et al., 2002a; De Busserolles et al., 2009; Fiala-Medioni et al., 2002; Halary et al., 2008; Trask and Van Dover, 1999). Experimentally, the abundance of endosymbionts has been shown to be linked to the presence or absence of substrate (Riou et al., 2010a, 2008). Our study lends further support to the high in situ trophic flexibility of *B. azoricus* across vent fields that is directly linked to the concentration of reduced compounds. Because SIA integrate diet information according to a time period dependant on tissue turnover, these results suggest that *B. azoricus* mussels are associated with a relatively constant niche. Although *B. azoricus* trophic flexibility is assumed to confer advantages for the colonization of a wide range of habitats, once established, these mussels may benefit from relatively stable environmental conditions over relatively long periods. The MAR is a slow and relatively young spreading centre (Desbruyères et al., 2001; Lalou, 1991) and temporal stability of vent communities can last for more than 14 years on the Eiffel Tower edifice in LS (Cuvelier et al., 2011). Overall, species shared across assemblages appeared to exhibit high trophic flexibility, adapting to the variation in basal sources. Interestingly, intra-field variability among distinct assemblages of the same edifice can be higher than inter-field variability observed for a single assemblage type. This trophic flexibility suggests weak trophic links to the metabolic diversity of chemosynthetic primary producers, which also may be a key to their adaptation to environmental variability between and within ecosystems. Our study thus lends further support to the hypothesis that exogenous rather than endogenous factors explain the dissimilarity in faunal community structure among northern MAR hydrothermal vents (Sarrazin et al., in preperation).

4.2. Functional complexity

At the community level, detritivores that include non-selective feeding strategies and bacterivorous specialists were identified as dominant whereas predators were poorly represented. Most of the few predators were generalists rather than specialists, as often reported for chemosynthetic ecosystems (Bergquist et al., 2007; Cordes et al., 2010a; Portail et al., 2016). Baseline-corrected δ^{15}N at the community level (representing the mean trophic level) was higher at LS_M than at RB_M, MG_G and RB_S, with MG_M being intermediate. Inter-assemblage variability of trophic guilds showed a higher dominance of detritivores and “commensals/parasites” in LS_M, a higher dominance of predators in RB_M whereas MG_M and MG_G as well as RB_S were almost exclusively composed of bacterivores. Higher fluid fluxes are usually associated with higher chemosynthetic primary production (Guezennec et al., 1998; LaMontagne et al., 2004; Sievert et al., 2000) and may thus provide more abundant food sources in RB_S and MG_G assemblages, which are located in habitats of high fluid intensity. Furthermore, among heterotrophs, the clear dominance of deposit-feeders compared with filter-feeders, supported the hypothesis that sessile free-living microorganisms are key players in the nutrition of the vent fauna, even in diffuse flow habitats, as previously suggested (Bergquist et al., 2007).

Addressing species trophic guilds and trophic links based on SIA includes several potential biases due to isotope routines, incorporation rates and fractionation factors of consumers (reviewed in Martínez del Rio et al., 2009). Furthermore, we identified, within vent assemblages, the presence of multiple δ^{15}N baselines, which may be an additional source of bias. Although most species rely on local production, non-specialized detritivores depending at least partially on photosynthetic-OM may, for example, have δ^{15}N signatures similar to those of predators. Likewise, although most taxa are heterotrophs that rely on free-living chemosynthetic microbial production, the δ^{15}N signatures of species relying at least partially on *B. azoricus* may be comparable or even depleted relative to primary consumers. For example, the crab *Segonzacia mesatlantica* is a potential detritivore/scavenger and predator of shrimp, amphipods and mussels (Table S2). In our study, its low δ^{15}N similar to microbial mats appears to reflect a highly specialized bacterivorous diet but also partial predation on *B. azoricus* tissues or its commensal polynoids. *In situ* observations of *S. mesatlantica* feeding on mussels tends to confirm their predation on *B. azoricus* (J. Sarrazin, personal observations, video Supplemental material 2 of Matabos et al., 2015). Therefore, despite its low δ^{15}N, *S. mesatlantica* was herein not assigned to a bacterivore specialist but rather to a mixotroph (detritivore/scavenger and predator). In addition, some taxa, known as bacterivores or detritivores, exhibited negligible or very low δ^{15}N enrichment compared with microbial mats, e.g. *Aphotopontius* sp. copepods, isopods and amphipods. These low δ^{15}N values, relative to other primary consumers, may result either from their belonging to distinct niches in which the δ^{15}N of primary producer may differ or from their weak trophic fractionation factors toward sources (< 3.4‰, Conway et al., 1994). In any case, the δ^{15}N variability among heterotrophic primary consumers can induce a bias in trophic guild assignment, because predators of such depleted consumers (i.e. secondary consumers) can have δ^{15}N signatures comparable to primary consumers. For example, *B. azoricus* larvae PII had a δ^{15}N signature comparable to that of some bacterivores or detritivores in their assemblages. However, the δ^{15}N of *B. azoricus* larvae PII may also reflect their predation on bacterivores that have low δ^{15}N. Further, at all sites where copepods where sampled (MG_{M1}, MG_{M2} and MG_{M3}, LS_{M1} and LS_{M2}), *B. azoricus* larvae PII had similar δ^{13}C and enriched δ^{15}N corresponding to one trophic level (MG: 2.4–4.4‰, LS: 3.6–5.5‰) with respect to *Aphotopontius* sp. copepods, thus suggesting a predator-prey link. The observation of *B. azoricus* larvae PII feeding on living *Aphotopontius* sp. (Video S1) further supports this predator-prey relationship and a heterotrophic diet in *B. azoricus* larvae. Without these faunal observations and recurrent SIA shifts between the two species, the larvae would have been classified as bacterivores. Overall, SIA need to be interpreted with caution based on the local δ^{15}N signatures of basal sources, species ecology, in situ observations of faunal interactions and the resulting hypotheses may be further explored using complementary approaches such as fatty acid or amino acid analyses.

Supplementary material related to this article can be found online at http://dx.doi.org/10.1016/j.dsr.2017.11.010.

Stable isotope ratios integrate a high degree of heterogeneity reflecting the complexity of ecological networks. Species' distributions in bidimensional isotopic space (δ^{13}C and δ^{15}N) effectively depend on their trophic diets and habitats, thus theoretically reflecting the concept of species ecological niche (Newsome et al., 2007) or the “realized” species trophic niche (Bearhop et al., 2004; Dubois and Colombo, 2014). Within chemosynthetic ecosystems, we may have the opportunity to assess habitat components even at microscales within assemblages, as demonstrated by the presence of multiple baselines (this study; Portail et al., 2016).

Quantification of the food web complexity based on SIA was addressed in mussel assemblages from the MG and LS vent fields. These assemblages are characterized by distinct environmental conditions (physico-chemical factors and basal sources) and faunal community structure (diversity and composition). Based on the temperature profile in the water column, MG is assumed to belong to a different water mass than LS (Schlitzer, 2000), affecting hydrodynamism or ambient temperatures for example. The two vent fields are characterized by distinct fluid compositions (Charlou et al., 2002; Le Bris and Duperron, 2010) as evidenced by methane and metal concentrations as well as the expected concentrations of hydrogen sulphide above mussel assemblages. According to these variations in fluid properties, the composition and metabolism of the microbiomes are assumed to differ between MG_M and LS_M (Cerqueira et al., 2017). The composition and diversity of the macrofaunal community in mussel beds are different between the two assemblages. Rarefied alpha diversity (ES_{215}) was two-fold higher at LS_M (11.2 ± 0.1) than MG_M (5.1 ± 0.8) (Sarrazin et al., in preparation). Faunal composition at MG_M was characterized by a high dominance of *P. valvatoides* and *L. atlanticus* gastropods whereas LS_M was dominated by *Branchipolynoe seepensis*, dorvilleids, and nemerteans. Composition dissimilarity was estimated at 68% between LS_M and MG_M and was mainly related to species turnover (50%) whereas nestedness was lower (18%). Despite these abiotic and biotic specificities of the two assemblages between vent fields, the structure of their food webs was similar. Layman's metrics quantifying the functional diversity, basal source diversification, trophic level length as well as the degree of specialization and redundancy did not differ between LS_M and MG_M. In addition, functional metrics that are biomass-dependant showed that the isotopic divergence, dispersion and redundancy within communities were also highly similar. This similarity in the structure of food webs despite previously introduced abiotic and biotic differences raises the question of the identification of ecological factors involved. The two assemblages were dominated by *B. azoricus* and thus shared the same environmental settings that define the niche of the mussel. Within this environmental setting, the physico-chemical discrepancies related to the nature of the fluid did not seem to influence the functional structure of the assemblages. This functional similarity may be favoured by the high ability of the common fauna to adapt to the spatially and temporally variable nature of fluids. Similarly, the influence of variation in microbial metabolism may also be relatively low because vent fauna appear to benefit from high trophic flexibility (this study; Bell et al., 2016; Levin et al., 2009; Portail et al., 2016). The stability of functional structure in communities that are characterized by distinct taxonomic composition and alpha diversity brings new insights with respect to the pattern described in a previous study using a similar analytical approach of food webs (Portail et al., 2016). In that study, assemblages dominated by the same foundation species in two different ecosystems (i.e. cold seep and hydrothermal vent) had comparable functional structure as well as comparable macrofaunal community composition. Herein, we suggest that the two different pools of species at MG_M and LS_M may play similar roles in the functional structure of the community. Different species may also have redundant functions across vent fields such that the high species turnover between communities is not coupled to functional turnover. Beyond these hypotheses, the influence of diversity on functional structure is relatively ambiguous and unexpected. In ecosystems where species sorting is assumed to play a primary role (Beinart et al., 2012; Cordes et al., 2010c; Govenar et al., 2015; Levesque et al., 2003; Levin et al., 2015, 2013; Portail et al., 2016), the increase in diversity is expected to affect and complexify the functional structure of community. Increase in biodiversity along a gradient of decreasing fluid flow has been associated to the complexification of the food web where high niche partitioning would be required for species coexistence, resulting in high functional diversity and specialization, but low redundancy (Portail et al., 2016). Our results suggest that for common assemblages (herein *B. azoricus*), that have similar fluid-flux settings, other processes may be involved. We suggest that the absence of a relationship between the functional structure and taxonomic diversity indicates that several co-occuring species have redundant functions. Accordingly, many species showed high variability in their isotopic signatures, leading to a great overlap among heterotrophic taxa within a community. Therefore, adding species within in a functional group, may not necessarily lead to more complexity. Interestingly, the highest variation in functional metrics was observed among samples within vent fields rather than between vent fields even though the environment and the structure of the faunal community (composition and diversity) were relatively similar. Trophic and habitat partitioning among functional groups may be of primary interest in the complexification of food webs at small spatial scale within chemosynthetic ecosystems. Accordingly, individuals belonging to the same species showed significant differences in SIA across samples. Environmental gradients in these assemblages are assumed to be relatively substantial and to affect faunal isotopic signatures, as demonstrated for the nitrogen ratios of endofauna from sediment (Portail et al., 2016) and suggested for epifauna from hard substrates with the presence of multiple baselines described in our MAR assemblages. Therefore, although fluid gradients shape the horizontal distribution of faunal assemblages, characterization of vertical gradients within assemblages appear to be an essential key to better assess food web patterns within chemosynthetic communities. Further work is needed to define the microdistribution of individuals within assemblages and their associated microhabitats (i.e. ecological optimum) to better assess species' ecological niches and biotic interactions.

Functional trait approaches have been developed to assess community patterns based on individual or species functions rather than species identity. Functional traits of species within chemosynthetic ecosystems are poorly known (Levin et al., 2016) and our study represents one of the first attempts to address functional complexity of vent assemblages. Our approach focuses on raw SI ratios (carbon source, trophic level and habitat), qualitative traits extracted from SI interpretation (trophic diet and strategy) as well as other qualitative functional traits of interest (size and mobility). The biomass-dependant functional metrics gave estimations of the functional divergence, dispersion and redundancy within communities. Of the three metrics, only one, i.e. the functional dispersion/specialization, differed significantly between the MG and LS mussel assemblages, with higher values at LS. Beyond $\delta^{13}C$ and $\delta^{15}N$, the functional traits analysis highlighted more heterogeneity in trait dominance for trophic guild, trophic strategy, size as well as mobility within LS. Associated with size and mobility, other functions (such as reproduction or dispersion strategies) can be depicted in the analysis and thus contribute to the higher variance observed compared to SIA-based metrics. Although these analyses provide interesting insights, more work is clearly needed to reach quantitative rather than qualitative approaches of species functional traits. Food-web studies have contributed substantially our knowledge of chemosynthetic ecosystem functioning, but functional traits should now be considered to reach a comprehensive view of the complexity there.

5. Conclusions

This food web study of MAR hydrothermal vent fields offers the opportunity to assess the functioning of vent communities at the regional scale, where both exogenous and endogenous factors can affect ecological processes. Contribution of photosynthetic-derived OM was negligible in all vent food webs and did not depend on vent-field depths. The dominant sources were related to methanotrophy and autotrophy using both the CBB and rTCA cycles and their contributions varied according to the availability in reduced compounds. Basal source dominance was influenced by environmental conditions, but species common to all assemblages appeared to exhibit high trophic flexibility, suggesting that the metabolic diversity of basal sources may not be a structuring factor. Diet variability was shown to be potentially higher between different assemblages within a given vent field than between common assemblages across vent fields. Further support was thus provided to the hypothesis that exogenous rather than endogenous factors explain the dissimilarity in faunal community structure between northern MAR hydrothermal vents. Food-web structure analysis at the community level showed that despite variation in environmental conditions and community structure, metrics of the functional structure were similar across assemblages. This functional similarity may be favoured by the low influence of the nature of fluids because vent fauna can adapt to several geological contexts and by the low influence of microbial metabolism due to the trophic flexibility of vent heterotrophs. In addition, ecological niches of the distinct species across vent fields may have similar role in the functional structure of the communities. Furthermore, different species may have redundant functions across ecosystems such that the high species turnover between two communities may not be coupled to a functional turnover at the community level. The absence of a relationship between functional and structural diversity, together with the presence of a high overlap between species isotopic niches within communities, also suggest that redundancy among co-occuring species is high. This species redundancy highlights that the addition of species within a functional group does not necessarily lead to more complexity. Overall, this study opens a new perspective on complexity within chemosynthetic communities and points to the need to better characterize species' ecological niches and biotic interactions.

Acknowledgements

We are grateful to the R/V *Pourquoi pas?* crew for their steadfast collaboration in the success of the BIOBAZ cruise, to the chief scientist of the cruise (Francois Lallier), to the *Victor 6000* submersible pilots for their patience and constant support and to the LEP technical staff for their valuable help both at sea and in the lab. This research received funding from the European Union Seventh Framework Programme (FP7/2007–2013) under the MIDAS project, grant agreement no. 603418. AC was supported by Program Investigador (IF/00029/2014/CP1230/CT0002) from the Fundação para a Ciência e Tecnologia (FCT). This study also benefited from the support of FCT through the strategic project UID/MAR/04292/2013 granted to MARE. The manuscript was professionally edited by Carolyn Engel-Gautier.

Appendix A. Supporting information

Supplementary data associated with this article can be found in the online version at http://dx.doi.org/10.1016/j.dsr.2017.11.010.

References

Allen, C.E., Copley, J.T., Tyler, P.A., 2001. Lipid partitioning in the hydrothermal vent shrimp Rimicaris exoculata. Mar. Ecol. 22 (3), 241–253.

Alperin, M.J., Reeburgh, W.S., Whiticar, M.J., 1988. Carbon and hydrogen isotope fractionation resulting from anaerobic methane oxidation. Glob. Biogeochem. Cycles 2 (3), 279–288.

Baker, M.C., Ramirez-Llodra, E., Tyler, P.A., German, C.R., Boetius, A., Cordes, E., Dubilier, N., Fisher, C., Levin, L.A., Metaxas, A., 2010. Biogeography, ecology and vulnerability of chemosynthetic ecosystems in the deep sea. In: McIntyre, A. (Ed.), Life in the World's Oceans: Diversity, Distribution, and Abundance. Blackwell Publishing Ltd, pp. 161–183.

Bearhop, S., Adams, C.E., Waldron, S., Fuller, R.A., MacLeod, H., 2004. Determining trophic niche width: a novel approach using stable isotope analysis. J. Anim. Ecol. 73 (5), 1007–1012.

Beinart, R.A., Sanders, J.G., Faure, B., Sylva, S.P., Lee, R.W., Becker, E.L., Gartman, A., Luther III, G.W., Seewald, J.S., Fisher, C.R., Girguis, P.R., 2012. Evidence for the role of endosymbionts in regional-scale habitat partitioning by hydrothermal vent symbioses. Proc. Natl. Acad. Sci. USA 109 (47), E3241–E3250.

Bell, J.B., Woulds, C., Brown, L.E., Sweeting, C.J., Reid, W.D.K., Little, C.T.S., Glover, A.G., 2016. Macrofaunal ecology of sedimented hydrothermal vents in the Bransfield Strait, Antarctica. Front. Mar. Sci. 3 (32).

Bergquist, D.C., Eckner, J.T., Urcuyo, I.A., Cordes, E.E., Hourdez, S., Macko, S.A., Fisher, C.R., 2007. Using stable isotopes and quantitative community characteristics to determine a local hydrothermal vent food web. Mar. Ecol. Progress. Ser. 330, 49–65.

Bode, A., Fernández, C., Mompeán, C., Parra, S., Rozada, F., Valencia-Vila, J., Viana, I.G., 2014. Differential processing of anthropogenic carbon and nitrogen in benthic food webs of A Coruña (NW Spain) traced by stable isotopes. Deep Sea Res. Part II: Top. Stud. Oceanogr. 106, 198–206.

Bourbonnais, A., Lehmann, M.F., Butterfield, D.A., Juniper, S.K., 2012. Subseafloor nitrogen transformations in diffuse hydrothermal vent fluids of the Juan de Fuca Ridge evidenced by the isotopic composition of nitrate and ammonium. Geochem. Geophys., Geosyst. 13 (2), 1525–2027.

Bremner, J., 2008. Species' traits and ecological functioning in marine conservation and management. J. Exp. Mar. Biol. Ecol. 366 (1–2), 37–47.

Brind'Amour, A., Dubois, S.F., 2013. Isotopic diversity indices: how sensitive to food web structure? PloS One 8 (12), e84198.

Brooks, J.M., Kennicutt, M., Fisher, C., Macko, S., Cole, K., Childress, J., Bidigare, R., Vetter, R., 1987. Deep-sea hydrocarbon seep communities: evidence for energy and nutritional carbon sources. Science 238 (4830), 1138–1142.

Campbell, B.J., Engel, A.S., Porter, M.L., Takai, K., 2006. The versatile [epsi]-proteobacteria: key players in sulphidic habitats. Nat. Rev. Microbiol. 4 (6), 458–468.

Carlier, A., Ritt, B., Rodrigues, C.F., Sarrazin, J., Olu, K., Grall, J., Clavier, J., 2010. Heterogeneous energetic pathways and carbon sources on deep eastern Mediterranean cold seep communities. Mar. Biol. 157 (11), 2545–2565.

Carney, R.S., 1994. Consideration of the oasis analogy for chemosynthetic communities at Gulf of Mexico hydrocarbon vents. Geo-Mar. Lett. 14 (2–3), 149–159.

Carney, R.S., 2005. Zonation of deep biota on continental margins. Oceanogr. Mar. Biol.: Annu. Rev. 43, 211–278.

Cavanaugh, C.M., Wirsen, C.O., Jannasch, H., 1992. Evidence for methylotrophic symbionts in a hydrothermal vent mussel (Bivalvia: Mytilidae) from the Mid-Atlantic ridge. Appl. Environ. Microbiol. 58 (12), 3799–3803.

Cerqueira, T., Pinho, D., Froufe, H., Santos, R.S., Bettencourt, R., Egas, C., 2017. Sediment microbial diversity of three deep-sea hydrothermal vents Southwest of the Azores. Microb. Ecol. 1–18.

Charlou, J., Donval, J., Fouquet, Y., Jean-Baptiste, P., Holm, N., 2002. Geochemistry of high H2 and CH4 vent fluids issuing from ultramafic rocks at the Rainbow hydrothermal field (36°14′ N, MAR). Chem. Geol. 191 (4), 345–359.

Charlou, J.L., Donval, J.P., Douville, E., Jean-Baptiste, P., Radford-Knoery, J., Fouquet, Y., Dapoigny, A., Stievenard, M., 2000. Compared geochemical signatures and the evolution of Menez Gwen (37°50′N) and Lucky Strike (37°17′N) hydrothermal fluids, south of the Azores Triple junction on the Mid-Atlantic ridge. Chem. Geol. 171 (1–2), 49–75.

Clark, J.S., 2016. Why species tell more about traits than traits about species: predictive analysis. Ecology 97 (8), 1979–1993.

Colaço, A., Dehairs, F., Desbruyeres, D., 2002a. Nutritional relations of deep-sea hydrothermal fields at the Mid-Atlantic Ridge: a stable isotope approach. Deep Sea Res. Part I: Oceanogr. Res. Pap. 49 (2), 395–412.

Colaço, A., Dehairs, F., Desbruyeres, D., Le Bris, N., Sarradin, P.M., 2002b. Delta C-13 signature of hydrothermal mussels is related with the end-member fluid concentrations of H2S and CH4 at the Mid-Atlantic ridge hydrothermal vent fields. Cah. Biol. Mar. 43 (3–4), 259–262.

Colaço, A., Desbruyères, D., Guezennec, J., 2007. Polar lipid fatty acids as indicators of trophic associations in a deep-sea vent system community. Mar. Ecol. 28 (1), 15–24.

Colaco, A., Prieto, C., Martins, A., Figueiredo, M., Lafon, V., Monteiro, M., Bandarra, N.M., 2009. Seasonal variations in lipid composition of the hydrothermal vent mussel *Bathymodiolus azoricus* from the Menez Gwen vent field. Mar. Environ. Res. 67 (3), 146–152.

Comeault, A., Stevens, C.J., Juniper, S.K., 2010. Mixed photosynthetic-chemosynthetic diets in vent obligate macroinvertebrates at shallow hydrothermal vents on volcano 1, South Tonga arc – evidence from stable isotope and fatty acid analyses. Cah. Biol. Mar. 51 (4), 351.

Conway, N., 1994a. Stable isotopes, microbial symbioses and microbial physiology. In: Lajtha, K., Michener, R. (Eds.), Stable Isotopes in Ecology and Environmental Science. Blackwell, pp. 158–186.

Conway, N., Kennicutt, M., Van Dover, C., 1994b. Stable isotopes in the study of marine chemosynthetic-based ecosystems. In: Lajtha, K., Michener, R. (Eds.), Methods in Ecology: Stable Isotopes in Ecology and Environmental Science. Blackwell Scientific, Oxford, UK, pp. 158–186.

Cordes, E.E., Becker, E.L., Fisherb, C.R., 2010a. Temporal shift in nutrient input to cold-seep food webs revealed by stable-isotope signatures of associated communities. Limnol. Oceanogr. 55 (6), 2537–2548.

Cordes, E.E., Becker, E.L., Hourdez, S., Fisher, C.R., 2010b. Influence of foundation species, depth, and location on diversity and community composition at Gulf of Mexico lower-slope cold seeps. Deep Sea Res. Part II: Top. Stud. Oceanogr. 57 (21), 1870–1881.

Cordes, E.E., Cunha, M.R., Galeron, J., Mora, C., Olu-Le Roy, K., Sibuet, M., Van Gaever, S., Vanreusel, A., Levin, L.A., 2010c. The influence of geological, geochemical, and biogenic habitat heterogeneity on seep biodiversity. Mar. Ecol. 31 (1), 51–65.

Crepeau, V., Bonavita, M.A.C., Lesongeur, F., Randrianalivelo, H., Sarradin, P.M., Sarrazin, J., Godfroy, A., 2011. Diversity and function in microbial mats from the lucky strike hydrothermal vent field. FEMS Microbiol. Ecol. 76 (3), 524–540.

Cucherousset, J., Villéger, S., 2015. Quantifying the multiple facets of isotopic diversity: new metrics for stable isotope ecology. Ecol. Indic. 56, 152–160.

Cuvelier, D., Sarrazin, J., Colaco, A., Copley, J., Desbruyeres, D., Glover, A.G., Tyler, P., Santos, R.S., 2009. Distribution and spatial variation of hydrothermal faunal assemblages at Lucky Strike (Mid-Atlantic Ridge) revealed by high-resolution video image analysis. Deep-Sea Res. Part I-Oceanogr. Res. Pap. 56 (11), 2026–2040.

Cuvelier, D., Sarrazin, J., Colaco, A., Copley, J.T., Glover, A.G., Tyler, P.A., Santos, R.S., Desbruyeres, D., 2011. Community dynamics over 14 years at the Eiffel tower hydrothermal edifice on the Mid-Atlantic ridge. Limnol. Oceanogr. 56 (5), 1624–1640.

de Bello, F., Lavorel, S., Díaz, S., Harrington, R., Cornelissen, J.C., Bardgett, R., Berg, M., Cipriotti, P., Feld, C., Hering, D., Martins da Silva, P., Potts, S., Sandin, L., Sousa, J., Storkey, J., Wardle, D., Harrison, P., 2010. Towards an assessment of multiple ecosystem processes and services via functional traits. Biodivers. Conserv. 19 (10), 2873–2893.

De Busserolles, F., Sarrazin, J., Gauthier, O., Gélinas, Y., Fabri, M.C., Sarradin, P.M., Desbruyères, D., 2009. Are spatial variations in the diets of hydrothermal fauna linked to local environmental conditions? Deep Sea Res. Part II: Top. Stud. Oceanogr. 56 (19–20), 1649–1664.

de Juan, S., Hewitt, J., Thrush, S., Freeman, D., 2015. Standardising the assessment of functional Integrity in benthic ecosystems. J. Sea Res. 98, 33–41.

Desbruyères, D., Almeida, A., Biscoito, M., Comtet, T., Khripounoff, A., Le Bris, N., Sarradin, P.M., Segonzac, M., 2000. A review of the distribution of hydrothermal vent communities along northern mid-Atlantic ridge: dispersal vs. environment controls. Hydrobiologia 440.

Desbruyères, D., Biscoito, M., Caprais, J.C., Colaco, A., Comtet, T., Crassous, P., Fouquet, Y., Khripounoff, A., Le Bris, N., Olu, K., Riso, R., Sarradin, P.M., Segonzac, M., Vangriesheim, A., 2001. Variations in deep-sea hydrothermal vent communities on the Mid-Atlantic Ridge near the Azores plateau. Deep-Sea Res. Part I-Oceanogr. Res. Pap. 48 (5), 1325–1346.

Detree, C., Chabenat, A., Lallier, F.H., Satoh, N., Shoguchi, E., Tanguy, A., Mary, J., 2016. Multiple I-type lysozymes in the hydrothermal Vent Mussel *Bathymodiolus azoricus* and their role in symbiotic plasticity. PloS One 11 (2), e0148988.

Dixon, R., Kahn, D., 2004. Genetic regulation of biological nitrogen fixation. Nat. Rev. Microbiol. 2 (8), 621–631.

Dubois, S., Colombo, F., 2014. How picky can you be? Temporal variations in trophic niches of co-occurring suspension-feeding species. Food Webs 1 (1), 1–9.

Duperron, S., Bergin, C., Zielinski, F., Blazejak, A., Pernthaler, A., McKiness, Z.P., DeChaine, E., Cavanaugh, C.M., Dubilier, N., 2006. A dual symbiosis shared by two mussel species, *Bathymodiolus azoricus* and *Bathymodiolus puteoserpentis* (Bivalvia: mytilidae), from hydrothermal vents along the northern Mid-Atlantic Ridge. Environ. Microbiol. 8 (8), 1441–1447.

Emerson, D., Rentz, J.A., Lilburn, T.G., Davis, R.E., Aldrich, H., Chan, C., Moyer, C.L., 2007. A novel lineage of proteobacteria involved in formation of marine Fe-oxidizing microbial mat communities. PloS One 2 (8), e667.

Feng, D., Cheng, M., Kiel, S., Qiu, J.-W., Yang, Q., Zhou, H., Peng, Y., Chen, D., 2015. Using *Bathymodiolus* tissue stable carbon, nitrogen and sulfur isotopes to infer biogeochemical process at a cold seep in the South China Sea. Deep Sea Res. Part I: Oceanogr. Res. Pap. 104, 52–59.

Fiala-Medioni, A., McKiness, Z.P., Dando, P., Boulegue, J., Mariotti, A., Alayse-Danet, A.M., Robinson, J.J., Cavanaugh, C.M., 2002. Ultrastructural, biochemical, and immunological characterization of two populations of the mytilid mussel *Bathymodiolus azoricus* from the Mid-Atlantic ridge: evidence for a dual symbiosis. Mar. Biol. 141 (6), 1035–1043.

Fisher, C., 1990. Chemoautotrophic and methanotrophic symbioses in marine-invertebrates. Rev. Aquat. Sci. 2 (3–4), 399–436.

Fisher, C.R., Childress, J.J., Macko, S.A., Brooks, J.M., 1994. Nutritional interactions in Galapagos Rift hydrothermal vent communities: inferences from stable carbon and nitrogen isotope analyses. Mar. Ecol. Progress. Ser. 103 (1–2), 45–55.

Fouquet, Y., Cambon, P., Etoubleau, J., Charlou, J.L., OndréAs, H., Barriga, F.J.A.S., Cherkashov, G., Semkova, T., Poroshina, I., Bohn, M., Donval, J.P., Henry, K., Murphy, P., Rouxel, O., 2013. Geodiversity of hydrothermal processes along the mid-atlantic ridge and ultramafic-hosted mineralization: a new type of oceanic Cu-Zn-Co-Au volcanogenic massive sulfide deposit. In: Rona, P.A., Devey, C.W., Dyment, J., Murton, B.J. (Eds.), Diversity of Hydrothermal Systems on Slow Spreading Ocean Ridges. American Geophysical Union, pp. 321–367.

Gage, J.D., 2004. Diversity in deep-sea benthic macrofauna: the importance of local ecology, the larger scale, history and the Antarctic. Deep Sea Res. Part II: Top. Stud. Oceanogr. 51 (14), 1689–1708.

Gebruk, A.V., Southward, E.C., Kennedy, H., Southward, A.J., 2000. Food sources, behaviour, and distribution of hydrothermal vent shrimps at the Mid-Atlantic ridge. J. Mar. Biol. Assoc. U. Kingd. 80 (3), 485–499.

Govenar, B., 2012. Energy transfer through food webs at hydrothermal vents: linking the lithosphere to the biosphere. Oceanography 25 (1), 246–255.

Govenar, B., Fisher, C.R., Shank, T.M., 2015. Variation in the diets of Hydrothermal vent gastropods. Deep Sea Res. Part II: Top. Stud. Oceanogr. 121, 193–201.

Gravel, D., Canham, C.D., Beaudet, M., Messier, C., 2006. Reconciling niche and neutrality: the continuum hypothesis. Ecol. Lett. 9 (4), 399–409.

Guezennec, J., Ortega-Morales, O., Raguenes, G., Geesey, G., 1998. Bacterial colonization of artificial substrate in the vicinity of deep-sea hydrothermal vents. FEMS Microbiol. Ecol. 26 (2), 89–99.

Halary, S., Riou, V., Gaill, F., Boudier, T., Duperron, S., 2008. 3D FISH for the quantification of methane- and sulphur-oxidizing endosymbionts in bacteriocytes of the hydrothermal vent mussel *Bathymodiolus azoricus*. ISME J. 2 (3), 284–292.

Hoch, M.P., Fogel, M.L., Kirchman, D.L., 1992. Isotope fractionation associated with ammonium uptake by a marine bacterium. Limnol. Oceanogr. 37 (7), 1447–1459.

Howarth, R.W., Marino, R., Lane, J., Cole, J.J., 1988. Nitrogen fixation in freshwater, estuarine, and marine ecosystems. 1. Rates and importance1. Limnol. Oceanogr. 33 (4part2), 669–687.

Hügler, M., Petersen, J.M., Dubilier, N., Imhoff, J.F., Sievert, S.M., 2011. Pathways of carbon and energy metabolism of the epibiotic community associated with the deep-sea hydrothermal vent shrimp *Rimicaris exoculata*. PloS One 6 (1), e16018.

Hügler, M., Sievert, S.M., 2011. Beyond the Calvin cycle: autotrophic carbon fixation in the ocean. Annu. Rev. Mar. Sci. 3, 261–289.

Hügler, M., Wirsen, C.O., Fuchs, G., Taylor, C.D., Sievert, S.M., 2005. Evidence for autotrophic CO_2 fixation via the reductive tricarboxylic acid cycle by members of the ε subdivision of proteobacteria. J. Bacteriol. 187 (9), 3020–3027.

Jackson, A.L., Inger, R., Parnell, A.C., Bearhop, S., 2011. Comparing isotopic niche widths among and within communities: SIBER–stable isotope bayesian ellipses in R. J. Anim. Ecol. 80 (3), 595–602.

Jaschinski, S., Hansen, T., Sommer, U., 2008. Effects of acidification in multiple stable isotope analyses. Limnol. Oceanogr.: Methods 6 (1), 12–15.

Jumars, P.A., Dorgan, K.M., Lindsay, S.M., 2015. Diet of worms emended: an update of polychaete feeding guilds. Annu. Rev. Mar. Sci. 7, 497–520.

Karl, D., 1995. Ecology of free-living, hydrothermal vent microbial communities. In: Karl, D. (Ed.), The Microbiology of Deep-sea Hydrothermal Vents. CRC Press, pp. 35–124.

Kato, S., Kobayashi, C., Kakegawa, T., Yamagishi, A., 2009. Microbial communities in iron-silica-rich microbial mats at deep-sea hydrothermal fields of the Southern Mariana Trough. Environ. Microbiol. 11 (8), 2094–2111.

Kennicutt, M., Burke, R., MacDonald, I., Brooks, J., Denoux, G., Macko, S., 1992a. Stable isotope partitioning in seep and vent organisms: chemical and ecological significance. Chem. Geol.: Isot. Geosci. Sect. 101 (3), 293–310.

Kennicutt, M.C., Burke, R.A., Macdonald, I.R., Brooks, J.M., Denoux, G.J., Macko, S.A., 1992b. Stable isotope partitioning in seep and vent organisms – chemical and ecological significance. Chem. Geol. 101 (3–4), 293–310.

Khripounoff, A., Vangriesheim, A., Crassous, P., Segonzac, M., Colaco, A., Desbruyeres, D., Barthelemy, R., 2001. Particle flux in the Rainbow hydrothermal vent field (Mid-Atlantic ridge): dynamics, mineral and biological composition. J. Mar. Res. 59 (4), 633–656.

Lalou, C., 1991. Deep-sea hydrothermal venting: a recently discovered marine system. J. Mar. Syst. 1 (4), 403–440.

LaMontagne, M.G., Leifer, I., Bergmann, S., Van De Werfhorst, L.C., Holden, P.A., 2004. Bacterial diversity in marine hydrocarbon seep sediments. Environ. Microbiol. 6 (8), 799–808.

Layman, C.A., Arrington, D.A., Montaña, C.G., Post, D.M., 2007. Can stable isotope ratios provide for community-wide measures of trophic structure? Ecology 88 (1), 42–48.

Le Bris, N., Duperron, S., 2010. Chemosynthetic communities and biogeochemical energy pathways along the Mid-Atlantic ridge: the case of *Bathymodiolus azoricus*. In: Rona, P., Devey, C., Dyment, J., Murton, B. (Eds.), Diversity of Hydrothermal Systems on Slow Spreading Ocean Ridges. American Geophysical Union, Washington, D. C, pp. 409–429.

Lee, R.W., Childress, J.J., 1996. Inorganic N assimilation and ammonium pools in a deep-sea mussel containing methanotrophic endosymbionts. Biol. Bull. 190 (3), 373–384.

Levesque, C., Juniper, S.K., Marcus, J., 2003. Food resource partitioning and competition among alvinellid polychaetes of Juan de Fuca ridge hydrothermal vents. Mar. Ecol. Progress. Ser. 246, 173–182.

Levin, L.A., Mendoza, G.F., Grupe, B.M., 2016. Methane seepage effects on biodiversity and biological traits of macrofauna inhabiting authigenic carbonates. Deep Sea Res. Part II: Top. Stud. Oceanogr.

Levin, L.A., Mendoza, G.F., Grupe, B.M., Gonzalez, J.P., Jellison, B., Rouse, G., Thurber, A.R., Waren, A., 2015. Biodiversity on the rocks: macrofauna inhabiting authigenic carbonate at Costa Rica methane seeps. PloS One 10 (7), e0131080.

Levin, L.A., Mendoza, G.F., Konotchick, T., Lee, R., 2009. Macrobenthos community structure and trophic relationships within active and inactive Pacific hydrothermal sediments. Deep Sea Res. Part II: Top. Stud. Oceanogr. 56 (19–20), 1632–1648.

Levin, L.A., Michener, R.H., 2002a. Isotopic evidence for chemosynthesis-based nutrition of macrobenthos: the lightness of being at Pacific methane seeps. Limnol. Oceanogr. 1336–1345.

Levin, L.A., Michener, R.H., 2002b. Isotopic evidence for chemosynthesis-based nutrition of macrobenthos: the lightness of being at Pacific methane seeps. Limnol. Oceanogr. 47 (5), 1336–1345.

Levin, L.A., Ziebis, W., Mendoza, G.F., Bertics, V.J., Washington, T., Gonzalez, J., Thurber, A.R., Ebbe, B., Lee, R.W., 2013. Ecological release and niche partitioning under stress: lessons from dorvilleid polychaetes in sulfidic sediments at methane seeps. Deep Sea Res. Part II: Top. Stud. Oceanogr. 92 (0), 214–233.

Limen, H., Juniper, S.K., 2006. Habitat controls on vent food webs at Eifuku volcano, Mariana arc. Cah. Biol. Mar. 47 (4), 449–455.

Luther, G.W., Rozan, T.F., Taillefert, M., Nuzzio, D.B., Di Meo, C., Shank, T.M., Lutz, R.A., Cary, S.C., 2001. Chemical speciation drives hydrothermal vent ecology. Nature 410 (6830), 813–816.

MacAvoy, S., Morgan, E., Carney, R., Macko, S., 2008. Chemoautotrophic production incorporated by heterotrophs in Gulf of Mexico hydrocarbon seeps: an examination of mobile benthic predators and seep residents. J. Shellfish Res. 27 (1), 153–161.

Macko, S.A., Fogel, M.L., Hare, P., Hoering, T., 1987. Isotopic fractionation of nitrogen and carbon in the synthesis of amino acids by microorganisms. Chem. Geol.: Isot. Geosci. Sect. 65 (1), 79–92.

Marcon, Y., Sahling, H., Borowski, C., dos Santos Ferreira, C., Thal, J., Bohrmann, G., 2013. Megafaunal distribution and assessment of total methane and sulfide consumption by mussel beds at Menez Gwen hydrothermal vent, based on geo-referenced photomosaics. Deep Sea Res. Part I: Oceanogr. Res. Pap. 75 (0), 93–109.

Martens, C.S., Albert, D.B., Alperin, M., 1999. Stable isotope tracing of anaerobic methane oxidation in the gassy sediments of Eckernforde Bay, German Baltic Sea. Am. J. Sci. 299 (7–9), 589–610.

Martínez del Rio, C., Wolf, N., Carleton, S.A., Gannes, L.Z., 2009. Isotopic ecology ten years after a call for more laboratory experiments. Biol. Rev. 84 (1), 91–111.

Martins, I., Colaco, A., Dando, P.R., Martins, I., Desbruyeres, D., Sarradin, P.-M., Marques, J.C., Serrao-Santos, R., 2008. Size-dependent variations on the nutritional pathway of *Bathymodiolus azoricus* demonstrated by a C-flux model. Ecol. Model. 217 (1–2), 59–71.

Matabos, M., Cuvelier, D., Brouard, J., Shillito, B., Ravaux, J., Zbinden, M., Barthelemy, D., Sarradin, P.M., Sarrazin, J., 2015. Behavioural study of two hydrothermal crustacean decapods: mirocaris fortunata and Segonzacia mesatlantica, from the Lucky Strike vent field (Mid-Atlantic Ridge). Deep Sea Res. Part II: Top. Stud. Oceanogr. 121, 146–158.

Mouchet, M.A., Villeger, S., Mason, N.W., Mouillot, D., 2010. Functional diversity measures: an overview of their redundancy and their ability to discriminate community assembly rules. Funct. Ecol. 24 (4), 867–876.

Newsome, S.D., Martinez del Rio, C., Bearhop, S., Phillips, D.L., 2007. A niche for isotopic ecology. Front. Ecol. Environ. 5 (8), 429–436.

O'Brien, C.E., Giovannelli, D., Govenar, B., Luther, G.W., Lutz, R.A., Shank, T.M., Vetriani, C., 2015. Microbial biofilms associated with fluid chemistry and megafaunal colonization at post-eruptive deep-sea hydrothermal vents. Deep Sea Res. Part II: Top. Stud. Oceanogr. 121, 31–40.

Olu, K., Cordes, E.E., Fisher, C.R., Brooks, J.M., Sibuet, M., Desbruyeres, D., 2010. Biogeography and potential exchanges among the Atlantic equatorial belt cold-seep faunas. PloS One 5 (8), e11967.

Parnell, A., Inger, R., Bearhop, S., Jackson, A., 2008. Stable Isotope Analysis in R (SIAR).

Parnell, A., Jackson, A., 2013. Stable Isotope Analysis in R. R package Version 4.2.

Parnell, A.C., Inger, R., Bearhop, S., Jackson, A.L., 2010. Source partitioning using stable isotopes: coping with too much variation. PloS One 5 (3), e9672.

Petersen, J.M., Zielinski, F.U., Pape, T., Seifert, R., Moraru, C., Amann, R., Hourdez, S., Girguis, P.R., Wankel, S.D., Barbe, V., 2011. Hydrogen is an energy source for hydrothermal vent symbioses. Nature 476 (7359), 176–180.

Pond, D.W., Dixon, D.R., Bell, M.V., Fallick, A.E., Sargent, J.R., 1997. Occurrence of 16:2(n-4) and 18:2(n-4) fatty acids in the lipids of the hydrothermal vent shrimps *Rimicaris exoculata* and *Alvinocaris markensis*: nutritional and trophic implications. Mar. Ecol. Progress. Ser. 156, 167–174.

Ponnudurai, R., Kleiner, M., Sayavedra, L., Petersen, J.M., Moche, M., Otto, A., Becher, D., Takeuchi, T., Satoh, N., Dubilier, N., Schweder, T., Markert, S., 2016. Metabolic and physiological interdependencies in the Bathymodiolus azoricus symbiosis. ISME J.

Ponsard, J., Cambon-Bonavita, M.-A., Zbinden, M., Lepoint, G., Joassin, A., Corbari, L., Shillito, B., Durand, L., Cueff-Gauchard, V., Compère, P., 2013. Inorganic carbon fixation by chemosynthetic ectosymbionts and nutritional transfers to the hydrothermal vent host-shrimp *Rimicaris exoculata*. ISME J. 7 (1), 96–109.

Portail, M., Olu, K., Dubois, S.F., Escobar-Briones, E., Gelinas, Y., Menot, L., Sarrazin, J., 2016. Food-Web Complexity in Guaymas Basin Hydrothermal Vents and Cold Seeps. PloS One 11 (9), e0162263.

Post, D.M., 2002. Using stable isotopes to estimate trophic position: models, methods, and assumptions. Ecology 83 (3), 703–718.

Rieley, G., Van Dover, C.L., Hedrick, D.B., Eglinton, G., 1999. Trophic ecology of *Rimicaris exoculata*: a combined lipid abundance stable isotope approach. Mar. Biol. 133 (3), 495–499.

Rigolet, C., Thiébaut, E., Brind'Amour, A., Dubois, S.F., 2015. Investigating isotopic functional indices to reveal changes in the structure and functioning of benthic communities. Funct. Ecol. 29 (10), 1350–1360.

Riou, V., Bouillon, S., Serrao Santos, R., Dehairs, F., Colaco, A., 2010a. Tracing carbon assimilation in endosymbiotic deep-sea hydrothermal vent Mytilid fatty acids by C-13-fingerprinting. Biogeosciences 7 (9), 2591–2600.

Riou, V., Colaco, A., Bouillon, S., Khripounoff, A., Dando, P., Mangion, P., Chevalier, E., Korntheuer, M., Santos, R.S., Dehairs, F., 2010b. Mixotrophy in the deep sea: a dual endosymbiotic hydrothermal mytilid assimilates dissolved and particulate organic matter. Mar. Ecol. Progress. Ser. 405, 187–201.

Riou, V., Duperron, S., Halary, S., Dehairs, F., Bouillon, S., Martins, I., Colaco, A., Santos, R.S., 2010c. Variation in physiological indicators in Bathymodiolus azoricus (Bivalvia: Mytilidae) at the Menez Gwen Mid-Atlantic ridge deep-sea hydrothermal vent site within a year. Mar. Environ. Res. 70 (3–4), 264–271.

Riou, V., Halary, S., Duperron, S., Bouillon, S., Elskens, M., Bettencourt, R., Santos, R.S., Dehairs, F., Colaco, A., 2008. Influence of CH4 and H2S availability on symbiont distribution, carbon assimilation and transfer in the dual symbiotic vent mussel Bathymodiolus azoricus. Biogeosciences 5 (6), 1681–1691.

Robinson, J.J., Polz, M.F., Fiala-Medioni, A., Cavanaugh, C.M., 1998. Physiological and immunological evidence for two distinct C-1-utilizing pathways in *Bathymodiolus puteoserpentis* (Bivalvia: mytilidae), a dual endosymbiotic mussel from the Mid-Atlantic Ridge. Mar. Biol. 132 (4), 625–633.

Rodrigues, C.F., Hilário, A., Cunha, M.R., 2013. Chemosymbiotic species from the Gulf of Cadiz (NE Atlantic): distribution, life styles and nutritional patterns. Biogeosciences 10 (4), 2569–2581.

Rybakova, E., Galkin, S., 2015. Hydrothermal assemblages associated with different foundation species on the East Pacific rise and Mid-Atlantic ridge, with a special focus on mytilids. Mar. Ecol. 36, 45–61.

Sahling, H., Galkin, S.V., Salyuk, A., Greinert, J., Foerstel, H., Piepenburg, D., Suess, E., 2003. Depth-related structure and ecological significance of cold-seep communities – a case study from the Sea of Okhotsk. Deep Sea Res. Part I: Oceanogr. Res. Pap. 50 (12), 1391–1409.

Salerno, J.L., Macko, S.A., Hallam, S.J., Bright, M., Won, Y.-J., McKiness, Z., Van Dover, C.L., 2005. Characterization of symbiont populations in life-history stages of mussels from chemosynthetic environments. Biol. Bull. 208 (2), 145–155.

Sarrazin, J., Legendre, P., De Busserolles, F., Fabri, M.-C., Guilini, K., Ivanenko, V.N., Morineaux, M., Vanreusel, A., Sarradin, P.-M., 2015. Biodiversity patterns, environmental drivers and indicator species on a High-temperature Hydrothermal edifice, mid-Atlantic ridge. Deep Sea Res. Part II: Top. Stud. Oceanogr. 121, 177–192.

Sarrazin, J., Portail, M., Cathalot, C., Laes, A., Husson, B., Le grand, E.,Sarradin, P.M., 2017. Intra- and inter-field variations in *Bathymodiolus azoricus* deep-sea faunal assemblages along the northern Mid Atlantic Ridge (In preparation).

Sarrazin, J., Robigou, V., Juniper, S.K., Delaney, J.R., 1997. Biological and geological dynamics over four years on a high-temperature sulfide structure at the Juan de Fuca Ridge hydrothermal observatory. Mar. Ecol. Progress. Ser. 153, 5–24.

Schlitzer, R., 2000. Electronic atlas of WOCE hydrographic and tracer data now available. Eos Trans. Am. Geophys. Union 81 (5) (45-45).

Schmidt, C., Vuillemin, R., Le Gall, C., Gaill, F., Le Bris, N., 2008. Geochemical energy sources for microbial primary production in the environment of hydrothermal vent shrimps. Mar. Chem. 108 (1–2), 18–31.

Sievert, S.M., Hügler, M., Taylor, C.D., Wirsen, C.O., 2008. Sulfur oxidation at deep-sea hydrothermal vents. In: Dahl, C., Friedrich, C.G. (Eds.), Microbial Sulfur Metabolism. Springer, pp. 238–258.

Sievert, S.M., Ziebis, W., Kuever, J., Sahm, K., 2000. Relative abundance of Archaea and bacteria along a thermal gradient of a shallow-water hydrothermal vent quantified by rRNA slot-blot hybridization. Microbiology 146 (6), 1287–1293.

Southward, E.C., Gebruk, A., Kennedy, H., Southward, A.J., Chevaldonne, P., 2001. Different energy sources for three symbiont-dependent bivalve molluscs at the Logatchev hydrothermal site (Mid-Atlantic ridge). J. Mar. Biol. Assoc. UK 81 (04), 655–661.

Spiridonova, E., Kuznetsov, B., Pimenov, N., Tourova, T., 2006. Phylogenetic characterization of endosymbionts of the hydrothermal vent mussel *Bathymodiolus azoricus* by analysis of the 16S rRNA, cbbL, and pmoA genes. Microbiology 75 (6), 694–701.

Stevens, C.J., Juniper, S.K., Limén, H., Pond, D.W., Metaxas, A., Gélinas, Y., 2015. Obligate hydrothermal vent fauna at East Diamante submarine volcano (Mariana Arc) exploit photosynthetic and chemosynthetic carbon sources. Mar. Ecol. Progress. Ser. 525, 25–39.

Trask, J.L., Van Dover, C.L., 1999. Site-specific and ontogenetic variations in nutrition of mussels (*Bathymodiolus* sp.) from the Lucky Strike hydrothermal vent field, Mid-Atlantic Ridge. Limnol. Oceanogr. 44 (2), 334–343.

Tunnicliffe, V., 1991. The biology of hydrothermal vents – ecology and evolution. Oceanogr. Mar. Biol. 29, 319–407.

Van Dover, C.L., 2007. Stable isotope studies in marine chemoautotrophically based ecosystems: anupdate. In: Michener, R., Lajtha, K. (Eds.), Stable Isotopes in Ecology and Environmental Science. Blackwell Publishing Ltd, pp. 202–237.

Van Dover, C.Lv, Fry, B., 1994. Microorganisms as food resources at deep-sea hydrothermal vents. Limnol. Oceanogr. 39 (1), 51–57.

Villéger, S., Mason, N.W., Mouillot, D., 2008. New multidimensional functional diversity indices for a multifaceted framework in functional ecology. Ecology 89 (8), 2290–2301.

Wei, C.-L., Rowe, G.T., Hubbard, G.F., Scheltema, A.H., Wilson, G.D., Petrescu, I., Foster, J.M., Wicksten, M.K., Chen, M., Davenport, R., 2010. Bathymetric zonation of deep-sea macrofauna in relation to export of surface phytoplankton production. Mar. Ecol. Progress. Ser. 399, 1–14.

Won, Y.-J., Hallam, S.J., O'Mullan, G.D., Pan, I.L., Buck, K.R., Vrijenhoek, R.C., 2003. Environmental acquisition of thiotrophic endosymbionts by deep-sea mussels of the genus *Bathymodiolus*. Appl. Environ. Microbiol. 69 (11), 6785–6792.

Zbinden, M., Le Bris, N., Gaill, F., Compère, P., 2004. Distribution of bacteria and associated minerals in the gill chamber of the vent shrimp *Rimicaris exoculata* and related biogeochemical processes. Mar. Ecol. Progress. Ser. 284, 237–251.

Zeebe, R.E., Wolf-Gladrow, D.A., 2001. CO_2 in Seawater: Equilibrium, Kinetics, Isotopes. Gulf Professional Publishing.